REPORT DOCUMENTATION PAGE

Form Approved
OMB No. 0704-0188

(2)

1.AGENCY USE ONLY	2.REPORT DATE	3.REPORT TYPE AND DATES COVER
	January 15, 1991	1 Oct 88 - 28 Feb 91 (Final)

4.TITLE AND SUBTITLE
DEVELOPMENT OF FINE-GRAINED, DUCTILE TUNGSTEN ALLOYS FOR ARMOR/ANTI-ARMOR APPLICATION

5.FUNDING NUMBERS
DAAL03-88-C-0031

6.AUTHOR(S)
J.P. Wittenauer and T.G. Nieh

7.PERFORMING ORGANIZATION NAMES(S) AND ADDRESS(ES)
Lockheed Missiles and Space Company, Inc.
Research and Development Division, O/9310, B/204
3251 Hanover Street, Palo Alto, Calfornia 94304

8.PERFORMING ORGANIZATION REPORT NUMBER
LMSC-F404866

9.SPONSORING/MONITORING AGENCY NAME(S) AND ADDRESS(ES)
U.S. Army Research Office
P.O. Box 12211
Research Triangle Park, NC 27709-2211

10.SPONSORING/MONITORING AGENCY REPORT NUMBER
ARO 26109.1-MS-A

11.SUPPLEMENTARY NOTES
The view, opinions and/or finding contained in this report are those of the author(s) and should not be construed as an official Department of the Army position, policy, or decision, unless as designated by other documentation.

12a.DISTRIBUTION/AVAILABILITY SATEMENT
Approve for public release; distribution unlimited.

12b.DISTRIBUTION CODE

13.ABSTRACT (*Maximum 200 words*)

The objective of this program has been to develop and enhance the ductility of tungsten-based materials at high strain rates through the control of microstructural parameters such as grain size, distribution of phases, and texture. The technical basis for this objective is the close relationship between fine-structure and extended plasticity in metals and ceramics. To obtain a fine and equiaxed grain structure in tungsten-based materials, a number of processing routes have been evaluated under this program. Based upon a critical evaluation of available processing schemes, four methods were selected to produce materials for detailed study. These processing methods included arc casting and thermomechanical processing of tungsten-based binary alloys, chemical vapor deposition, liquid phase sintering, and consolidation of ultrafine powder. These above methods have been used to produce fine-structure tungsten materials under this program and some physical and mechanical properties have been evaluated. An overview of the research program is presented together with a summary of the microstructures and properties of materials produced to date.

14.SUBJECT TERMS	15.NUMBER OF PAGES
tungsten, fine grains, sintering, microstructures, anti-armor, heavy alloy	60
	16.PRICE CODE

17.CLASSIFICATION OF REPORT	18.CLASSIFICATION OF THIS PAGE	19.CLASSIFICATION OF ABATRACT	20.LIMITATION OF ABSTRACT
unclassified	unclassified	unclassified	UL

LMSC-F404866

Lockheed
Research & Development Division

Final Report for Period

1 October, 1988 to 28 February 1991

DEVELOPMENT OF FINE-GRAINED, DUCTILE TUNGSTEN ALLOYS FOR ARMOR/ANTI-ARMOR APPLICATIONS

Prepared for:

U.S. ARMY RESEARCH OFFICE
Dr. Andy Crowson
Dr. Iqbal Ahmed

ARO Contract Number DAAL03-88-C-0031

Prepared by:

LOCKHEED MISSILES & SPACE COMPANY, INC.
J. Wittenauer and T.G. Nieh

15 January, 1991

DEVELOPMENT OF FINE-GRAINED, DUCTILE TUNGSTEN ALLOYS FOR ARMOR/ANTI-ARMOR APPLICATIONS

LMSC-F404866
15 January, 1991

LOCKHEED MISSILES & SPACE COMPANY, INC.
J. Wittenauer and T.G. Nieh

Abstract

The objective of this program has been to develop and enhance the ductility of tungsten-based materials at high strain rates through the control of microstructural parameters such as grain size, distribution of phases, and texture. The technical basis for this objective is the close relationship between fine-structure and extended plasticity in metals and ceramics. To obtain a fine and equiaxed grain structure in tungsten-based materials, a number of processing routes have been evaluated under this program. Based upon a critical evaluation of available processing schemes, four methods were selected to produce materials for detailed study. These processing methods included arc casting and thermomechanical processing of tungsten-based binary alloys, chemical vapor deposition, liquid phase sintering, and consolidation of ultrafine powder. These above methods have been used to produce fine-structure tungsten materials under this program and some physical and mechanical properties have been evaluated. An overview of the research program is presented together with a summary of the microstructures and properties of materials produced to date.

Contents

1.0 Introduction

Tungsten-based alloy systems have been considered for armor-defeating projectile applications for a number of years because of their high density and low cost relative to other refractory metals. Tungsten (W) also does not pose the health hazard that is found with depleted uranium alloys. As a result, tungsten-based alloys have been tried in small and medium caliber ammunition, in long rod kinetic energy penetrators, and as the liners in shaped charge warheads.

The development of W-based anti-armor systems, however, has been hindered by their inherent brittleness. For example, tungsten alloy kinetic energy penetrators can fracture upon launch or can fracture into several pieces at impact, rendering them less effective against multiple layer targets. Tungsten alloy shaped charge liners particulate very early on in the jet formation process, again substantially reducing their effectiveness. Clearly, to increase the performance of tungsten alloys in anti-armor applications, ways must be found, either through microstructural or compositional control, to increase the ductility and/or fracture toughness of tungsten at high loading rates.

The objective of this program was to develop and enhance the ductility of tungsten alloys at high strain rates through control of microstructural parameters such as grain size, distribution of phases, and texture. The overall approach has been to use thermomechanical processing, deposition methods, and advanced powder metallurgy techniques to achieve the desired microstructural characteristics.

The technical basis for this research program lies in the relationship between microstructure and extended plasticity in metals and ceramics. In particular, the phenomenon of superplasticity in metals and ceramics has been shown to be directly correlated with fine grain size. High strain rate superplasticity has been observed in mechanically alloyed nickel-based materials, mechanically alloyed aluminum-based materials, and a particulate reinforced aluminum material [1-3]. In this study, it has been the goal to extend these results to tungsten-based materials. The main technical issue for the investigation of extended plasticity in tungsten-based materials,

therefore, is how to produce a fine grained, thermally stable microstructure.

To address this technical issue, a number of processing routes have been considered and several selected for the production of W-based materials. The processing routes considered are summarized below as a number of specific program tasks.

2.0 *Program Tasks*

The objective of this program was to produce tungsten-based materials which exhibited a uniform fine grain size, fine dispersoid distribution, or a fine two-phase microstructure. A number of specific tasks to accomplish this objective are summarized below.

TASK I: FINE STRUCTURE IN BULK MATERIALS

Task IA: Thermomechanical Processing of Commercially Available Oxide Dispersion Strengthened (ODS) Tungsten

The objective of this task was to consider methods of obtaining a fine equiaxed grain size in commercially available ODS tungsten. Typically, ODS-tungsten alloys are prepared by the mixing of tungsten powder with a thoria dispersoid, consolidated by electrical resistance sintering at temperatures in excess of 2000° C, and finally densified through elevated temperature swaging or forging. Since the swaging and forging treatments used involve unidirectional processing of the material, a microstructure is produced which exhibits elongated grains. By considering alternative means of thermomechanical processing, it was expected that a more desirable equiaxed microstructure could be produced.

Task IB: Casting and Thermomechanical Processing of Tungsten-Based Binary Alloys

The addition of alloy elements to W offers an alternative method to obtain fine structures and potentially enhanced ductility in W. An example of such an approach is the development of W-Re alloys which are already in use for various applications [4]. Unfortunately, the cost of Re has prohibited W-Re from wide usage. The objective of selecting a W-based binary alloy is to obtain a two phase microstructure which can be processed into a fine equiaxed grain structure. Ideally, a dilute amount of alloy additive should be used in order to avoid a decrease in density. A survey of W-X binary systems reveals several alloy systems of potential interest. The W-Hf, W-Zr, W-Os and W-Ir systems all exhibit terminal solid solubility with tungsten and decreasing solubility with temperature [5]. Dilute solid solutions made with these alloys could be processed to contain a fine dispersion of second phase through appropriate solutioning and ageing

treatments. Furthermore, mechanical deformation could be incorporated as precipitation occurs resulting in additional structure refinement. Unfortunately, Zr and Hf form brittle hydrides when exposed to hydrogen at elevated temperatures. This would be likely to render these alloys brittle since the only practical way to process W-based materials at elevated temperatures is through the use of hydrogen atmospheres. Alloying with Iridium or Osmium has not been seriously considered because of the relative scarcity of these metals.

Several W-X binary systems exhibit a continuous solid solubility at high temperatures and a solid state miscibility gap at low temperatures. Such characteristics offer an opportunity to obtain two-phase microstructures. Among the binary systems which exhibit these features are W-Ti and W-Cr. The W-Cr system is probably the best candidate for experimental evaluation. Tungsten-chromium alloys have a similar density, for equivalent alloy additions, as the conventional W-Ni-Fe heavy metals; they also have good oxidation resistance at temperatures up to 1000° C [6], and have a two-phase microstructure up to 1495° C [7]. Additionally, W-Cr alloys have been shown to exhibit good hot workability [8]. Because of their good oxidation resistance, it is anticipated that such alloys can be thermomechanically processed in air with minimal precaution for protective atmosphere during material handling.

Although not extensively studied in this program, W-based ternary systems may be of interest in obtaining a fine-structure material. The goal would be to find a ternary composition, high in W content, which exhibits a precipitation or eutectoid reaction at a temperature in the range of 1000°C-1500°C. At higher temperatures, it is impractical to mechanically work the alloy, while at lower temperatures, the kinetics of phase formation may be too slow to be of value. Unfortunately, W-based ternary phase diagrams have been determined for only a limited number of systems. Thus, it was not possible to fully study the merits of this approach at the present time.

Task IC: Fine Structure via Chemical Vapor Deposition

Production of tungsten sheet via chemical vapor deposition offers an alternative processing route for obtaining fine grain size. Chemical vapor deposition of tungsten is achieved by the hydrogen reduction of tungsten hexafluoride and deposition onto a suitable substrate. The deposition process results in a highly textured material, and often columnar grains are present. Previous reports indicate that CVD-tungsten sheet can be thermomechanically processed to modify the as-deposited grain structure [9]. Additionally, novel processing techniques have emerged which yield a fine-structure material by interupting the growth of columnar grains. The goal of this task has been to evaluate CVD tungsten from a number of sources and, based upon microstructural considerations, select the most promising material for further studies.

TASK II: FINE STRUCTURE VIA POWDER PROCESSING

Task IIA: Consolidation of Tungsten via Liquid Phase Sintering

Consolidation of tungsten by the liquid phase sintering technique yields a material with a unique combination of density, ductility, high strength, and low thermal expansion coefficient. The most common method of sintering W involves the use of a Ni-Fe matrix. The material produced is essentially a composite material with grains of highly dense W embedded in a ductile Fe-Ni or Cu-Ni based matrix.

The liquid phase sintering of W-Ni-Fe and W-Ni-Cu has been extensively studied and is quite well understood [10-17]. Elemental powders are blended, cold compacted, and heated to a temperature sufficient for liquation of the Fe+Ni or Cu+Ni matrix. Liquid phase sintering is classically divided into three stages which often overlap one another [18,19]. The initial stage is one of particle rearrangement as the melt forms and is drawn by cappilary action into the pores among adjoining W grains. Capillary forces are strong enough at this stage to cause particle rearrangement and contraction of the powder compact. A second stage is denoted as the solution-reprecipitation stage. The high melting point solid partially dissolves into the liquid, is transported rapidly through the liquid, and is reprecipitated at energetically favorable sites on

adjoining solid particles. Because of the efficiency of liquid phase transport, particle coarsening and associated pore elimination occur rapidly during this stage. The final stage of liquid phase sintering is denoted as solid-state-controlled sintering and may involve the coalescence of adjoining solid grains, neck growth of contacting grains, and growth of any residual pores.

There are three requirements for successful liquid phase sintering and these may be deduced from a consideration of the above described sequence of events [18,19]. Firstly, a system must be chosen which has a low melting point liquid and a high volume fraction of high melting point solid. Secondly, the liquid must wet the solid particles upon liquation. Lastly, the solid particles must exhibit some degree of solubility in the liquid. The latter requirement is of particular importance if full density is to be achieved. For example, in the W-Ni-Fe system, the Ni-Fe solution - typically combined in a weight ratio of 7Ni:3Fe - dissolves 22% of W (by weight) into the liquid [20,21]. This provides a rapid means of W transport, W grain growth, and resultant pore elimination. The grain growth in the W-Ni-Fe system during liquid phase sintering can be substantial. Published reports indicate that initial tungsten powders in the size range of 2-5 μm may grow by a factor of ten or more during liquid phase sintering [12-15]. Similarly, for the W-Cu-Ni system, tungsten grains reportedly increase from a 3 μm initial diameter to a final diameter of 40-50 μm during liquid phase sintering [17].

Work to date on W-based heavy metals has emphasized the role of microstructural parameters in controlling the mechanical behavior of the as-sintered product. It has been demonstrated, for example, that the tensile failure of W-based heavy metals initiates at sites of W-W particle contact [13,15,21,22]. When local failure occurs by interparticle separation, the ductile matrix bears the remaining tensile load until final specimen failure occurs. For this reason, a higher fraction of matrix enhances ductility by providing less opportunity for W-W particle contact. Similarly, a low value for the dihedral angle[†]- an indicator of the amount

[†] The *Dihedral Angle* is the angle formed at the triple point junction of two solid grains and the liquid. It is an indicator of the ratio of the solid-solid surface energy to the solid-liquid surface energy in liquid phase sintered materials.

of liquid penetration between adjoining W grains - improves the tensile ductility. The improvement of mechanical properties has also been shown to be dependent upon suppressing the formation of brittle intermetallic phases at the W-matrix interface. Nickel and iron are commonly used in a weight ratio of 7:3 in W-Ni-Fe heavy metals in order to avoid the formation of brittle intermetallic phases [12]. As with all powder metallurgy processed materials, the mechanical properties are critically dependent upon porosity. For this reason, 100% theoretical density is always the processing goal.

An important microstructural characteristic which has received little attention in W-based heavy alloys is that of grain size. The effect of grain size on the mechanical behavior of metals was, historically, one of the earliest understood metallurgical phenomenon. Grain size determines the room temperature yield strength, has an important bearing on fracture mode of a material, and determines to a large extent the elevated temperature plasticity characteristics of a material. Because of rapid particle growth in W-Ni-Fe and W-Ni-Cu systems, grain size is not readily amenable to control by the materials scientist and a study of grain size effects has not been possible. It has been demonstrated, however, that the addition of alloying ingredients which reduce the solubility of W in the liquid can reduce the grain coarsening rate during sintering [20]. Additions of Mo or Ta to the W-Ni-Fe system were shown to reduce the level of grain growth and to yield materials exhibiting higher strengths but lower ductilities than the W-Ni-Fe baseline material. The increased strength in these systems was attributed to reduced grain size and solid solution strengthening of the W particles by the additive. Similarly, a decrease in the Ni to Cu ratio in W-Ni-Cu alloys restricts the degree of grain growth because of a decreasing solubility for W in the liquid matrix as the Ni content decreases [17].

In the present program, an alternative means of producing a fine-structure heavy alloy has been studied. Like the above cited work in limiting grain growth in W-based heavy alloys, it is recognized that grain growth can best be limited by inhibiting the transport of W through the liquid during sintering. To achieve this objective, a liquid is chosen which exhibits only a limited solubility for tungsten. The liquid chosen

for the present study is based on copper. The previously determined W-Cu equilibrium diagram indicates that liquid Cu exhibits no solubility for W [23]. Selection of Cu as the liquid matrix is therefore expected to completely eliminate particle coarsening via the mechanism of liquid phase transport. A previous report indicates that Co addition is useful in enhancing the sintering behavior in the W-Cu system though a detailed study of sintering behavior in this system has not been presented [24]. The objective of this task is to further explore the role of Co on the sintering behavior of the W-Cu-Co system and to elucidate those factors which enhance the densification of this material.

Task IIB: Consolidation of Tungsten via Solid State Sintering

The goal of this task was to consolidate tungsten powder to full density while maintaining a fine equiaxed grain size. The task is similar to Task IA in that an ODS-tungsten material was chosen for study. In this task, however, it was the intent to process the material from powder. Task IA was designed to thermomechanically process material which was already consolidated to full density. The material chosen for examination was W with 0.36% (weight) or 1.4% (volume) yttria. The dispersion was added so as to pin the grain boundaries during elevated temperature processing and thus, preserve the fine grain size of the starting powders. Yttria was chosen for a dispersion over the more commonly used thoria simply in order to provide information on an alternative, and possibly improved, material.

Task IIC: Fine Structure Through Use of Ultrafine (Nanometer) Powder

Recent advances in sol-gel processing have led to the availability of W powders of high purity in the nanometer size range. The availability of these powders presents a unique opportunity to achieve the technical objective of this research program. Overall, a series of tungsten powders have been procured which exhibit a size range spanning 4 orders of magnitude (0.02 μm to 150 μm). The goal of this task was to prepare fully dense materials from these powders via liquid phase sintering. The availability of fully dense materials having a grain size range of 4 orders of magnitude would ultimately lead to mechanical properties measurements which would clearly define the role of grain size in W-based materials.

3.0 *Progress*

TASK I: FINE STRUCTURE IN BULK MATERIALS

Task IA: Thermomechanical Processing of Commercially Available Oxide Dispersion Strengthened (ODS) Tungsten

The microstructures of W-2% ThO_2 (thoriated-W) from three suppliers have been evaluated. Microstructural examinations were carried out on as-sintered materials as well as on the fully dense swaged or extruded bar. The microstructure of as-sintered W-2% ThO_2 is shown in Figure 1. This material was sintered to 90% density at a temperature of 2200°C. To obtain full density, thermomechanical processing is required. Unfortunately, such processing results in coarsening of the thoria particles and elongation and growth of the W grains. A typical transverse cross section from a 30 mm diameter thoriated-W bar is shown in Figure 2. The microstructure obtained consists of coarse W grains and the dispersion of ThO_2 particles exhibits a wide range of size distribution, despite the fact that the starting ThO_2 powders are submicron in size. This suggests that coarsening and agglomeration have occurred during processing. The photomicrograph in Figure 1 shows a tungsten grain size in the range of 50 μm and an oxide dispersion with a size range of 1 to 10 μm. Shown in Figure 3 is the microstructure for a W-2% ThO_2 bar in the *longitudinal* direction. Both the W grains and the ThO_2 particles are elongated along the deformation direction. The microstructures shown in Figures 2 and 3 are typical of all commercially-available thoriated-W bars evaluated. A typical Vickers Hardness value for this material is 500 kg/mm^2.

The objective of Task 1 was to produce a fine equiaxed grain size (grain diameter of 5 μm or lower) in thoriated-W via thermomechanical processing. Alternative processing schemes such as low temperature deformation followed by a recrystallization anneal or hot working in a temperature range favorable for continuous dynamic recrystallization were considered as possible routes for accomplishing this task. These methods can be successful if the dispersion particles, ThO_2, are fine and stable during thermomechanical processing. Since the ThO_2 particles in the commercially available thoriated-W were coarsened during thermomechanical processing

however, it is anticipated that these ThO_2 particles would not be effective as sites for nucleation of new grains nor as effective barriers to prevent grain growth upon dynamic recrystallization. The development of new processing procedures, to replace existing ones, to minimize the coarsening and agglomeration of ThO_2 appears impractical. Swaging and forging schedules currently used by industry have been carefully adopted to avoid local cracking at sites of ThO_2 particles. As a result of these findings, further research on this task was suspended.

Task IB: Casting and Thermomechanical Processing of Tungsten-Based Binary Alloys

Efforts to produce a W-Cr alloy were hampered by the high melting point of the alloy and by the difference in vapor pressures between molten chromium and molten tungsten. Initially, alloy preparation by arc casting and electron beam melting were considered. Since electron beam melting is relatively expensive, the alloy was prepared by arc melting. Preliminary efforts to prepare W-Cr alloys by arc melting at Lockheed were partially successful. A 50 g cast button prepared from pure W is shown in Figure 4. Because of the high melting point of this material, an enormous amount of heat must be dissipated by the water-cooled copper hearth. Insufficient cooling during casting has, in the case shown, led to local melting of the copper hearth and also to contamination in the cast tungsten alloy. Even with increased cooling of the copper hearth, W-ThO_2 electrode continued to show evidence of melting and a high purity specimen could not be produced. Recently, W-Cr alloys were prepared by arc casting at Westinghouse Advanced Energy Systems, Pittsburgh PA, and supplied to this program. Preweighed quantities of Cr electrolytic flake and pure W sheet were used. Due to the high vapor pressure of Cr relative to that of W, only compositions low in Cr could be prepared. A composition composed of 4% (weight) Cr was successfully prepared while a second composition composed of 12% (weight) was difficult to make.

Consideration of the W-Cr phase diagram suggests that 4% Cr is sufficient to provide a substantial amount of Cr-rich precipitates. It is expected that fine grain size can be obtained in this alloy via thermomechanical processing in a manner which is analagous to the

processing schemes used to obtain fine grain size in materials such as HSLA steels, UHC steels, α-β titanium alloys, and many aluminum alloys. All of these materials are mechanically worked as they cool through a temperature regime in which a second phase is precipitating out of solid solution. Mechanical working provides favorable sites for precipitation, and dynamic recrystallization during working produces defect-free grains with precipitates lying at the grain boundaries. The precipitates act to pin the grains and coarsening is hindered.

The microstructure of the W-4% Cr alloy is shown in Figure 5. The material shown was prepared by solution annealing the arc-cast material for 40 hrs at 1400°C, rapidly cooling, and ageing at 1000°C for 2 hrs. Shown in Figure 5 is a coarse grain size, as expected for a cast material, and a fine distribution of Cr-rich precipitates. It is seen that different grains contain different concentrations of the precipitates. This suggests that complete chemical homogeneity may not have been achieved in the melting operation and subsequent long-term solution treatment. Nevertheless, the microstructure shown in Figure 5 is one which offers promise for producing a fine-structure tungsten via an appropriate thermomechanical processing route.

Task IC: Fine Structure via Chemical Vapor Deposition

Chemical vapor deposited tungsten plate was obtained from COMURHEX, France, for evaluation. Also, a cylindrical shell of CVD tungsten has been supplied to this program by Lawrence Livermore National Laboratory (LLNL). The material provided by LLNL is made by a process which involves brushing of the surface during deposition to continually interrupt the columnar growth texture in the deposit. Deposits prepared by this method would be expected to provide a fine grain size (less than 1 μm) and an equiaxed morpholoy. A microstructural comparison of the materials produced by LLNL and COMURHEX shows some differences. Microstructures from each of the CVD materials is shown in Figure 6 and Figure 7.

The microstructure from the CVD tungsten sheet prepared by COMURHEX is shown in Figure 6. The material appears to be fully dense and free from inclusions. The grain size is approximately 10 μm and there appears to be

a slight degree of growth texture present. The Vickers hardness of the COMURHEX CVD tungsten was 548 kg/mm^2. The material prepared at LLNL is shown in Figure 7. The grain structure is finer than that of the COMURHEX material although some degree of growth texture is evident in this material as well. The Vickers hardness of the Livermore CVD tungsten is 574 kg/mm^2. By comparison, wrought P/M tungsten sheet which we examined had a Vickers hardness of 514 kg/mm^2 (unrecrystallized) or 410 kg/mm^2 (recrystallized).

A preliminary study of the behavior of CVD tungsten prepared by LLNL has yielded useful information regarding the response of the material to heat treatment. Annealing of the CVD tungsten can be expected to alter the grain morphology and hardness, perhaps resulting in an enhancement of the mechanical properties of the material. A series of annealing experiments was conducted at 1000° C and 1400° C for times ranging up to 16 hrs. Some of the results of these studies are summarized below in Table I.

Table I

EFFECT OF ANNEALING TREATMENT ON CVD TUNGSTEN (LLNL MATERIAL)

Treatment	Time	Microhardness	Grain Morphology
As-recieved	---	574 kg/mm^2	2-5 μm width, 2:1 Aspect Ratio
1000°C	16 hrs	534	2-5 μm width, 2:1 Aspect Ratio
1400°C	4 hrs	518	2-5 μm width, 2:1 Aspect Ratio
1400°C	8 hrs	500	4-8 μm width, 2:1 Aspect Ratio

These data indicate that the grain structure of the LLNL CVD tungsten is quite stable. Even after annealing for an extended time at 1400° C, the microstructure remains relatively unchanged, although a slight drop in microhardness is observed. As mentioned earlier, the Livermore CVD tungsten was supplied in the form of a cylindrical shell having a diameter of 10 cm and a wall thickness of approximately 1.5 mm. To obtain tensile coupons and evaluate the mechanical properties of this material, it was necessary to section the cylinder and vacuum hot press at 1000°C to obtain a flat sheet. The data presented in Table I suggest that this procedure

should have had little effect upon the mechanical properties of the material.

In order to provide an understanding of the structure-property relationships for CVD tungsten sheet, tensile coupons were prepared from both the Livermore and COMURHEX CVD tungsten sheet materials. For comparison purposes, specimens were also prepared from commercially available P/M - source wrought W sheet. The specimens were prepared by electro discharge machining and are shown in Figure 8. Prior to tensile testing, all specimens were prepared by lapping through 25 μm SiC and electropolishing of the gauge section. A variety of tensile tests both at room temperature and at elevated temperatures, are planned but are no longer within the scope of this program.

TASK II: FINE STRUCTURE VIA POWDER PROCESSING

The experimental work carried out under Task II required the use of a wide range of powder processing equipment. The equipment assembled at Lockheed for dedicated use under this research program included:

- an inert atmosphere glove box for safe handling of powders
- a mechanical attritor with tungsten carbide balls for mechanical alloying of tungsten powders
- a die of appropriate geometry for cold compaction of prepared powders
- a high temperature sintering furnace with programmable temperature controller and temperature capability to 1600°C
- a thermoelectrically cooled optical dewpoint sensor to monitor moisture content of the process atmosphere
- a hydrogen purifier based upon silver-paladium cell technology to provide ultrapure hydrogen as a sintering atmosphere

During the initial stage of this program, significant efforts were devoted to constructing and modifying the necessary equipment. In the latter stage of the present program, great strides were made in determining the factors

which affect the sintering characteristics of W powders. The progress in the area of fine structure via powder processing is reported below.

Task IIA: Consolidation of Tungsten via Liquid Phase Sintering

All sintering experiments for this study were carried out with the high purity powders listed in Table II. Tungsten powder containing a dispersion of 1.4% (vol) Y_2O_3 was supplied by GTE-Sylvania. The powder was prepared by spray drying a salt solution of W containing 0.28% (weight) Y. This amount of Y, when converted to Y_2O_3, provides a total dispersoid content of 0.36% by weight or 1.4% by volume. The dried salt was converted to an oxide followed by hydrogen reduction to obtain the metallic powder. It is not expected that the hydrogen reduced the Y_2O_3. Chemical composition of the powder is listed in Table II. The powder has a mean particle size of 4.5 μm and representative powder is shown in the SEM micrograph of Figure 9. The powder morphology is blocky because of particle growth along crystallographic planes. The particle size distribution appears to be bimodal in nature with some large (5 μm) particles as well as a substantial fraction of fine (1 μm) particles.

In this program, many sintering experiments were carried out with a range of compositions, sintering parameters, and atmospheres. The principal experiments are summarized below. The results of these experiments provide a fairly complete summary of the sintering behavior in the W-Cu-Co system.

One objective of the current work was to study the effect of Co addition on the sintering behavior. Only the lower fractions of Co were chosen for study in order to preserve the ductile nature of the Cu matrix. Initial experiments involved the conventional blending of elemental powders in a shaker mill. For these experiments, preweighed mixtures of elemental powder were shaken in a planetary shaker mill for 30 minutes. Later experiments utilized mechanical alloying techniques to obtain a greater degree of mixing among the elemental powders. For the mechanically alloyed mixtures, preweighed quantities of elemental powders were placed in a tungsten carbide cannister and milled with tungsten carbide balls for one hour in a high-energy shaker mill. For all cases, a mass of 15 grams of

powder was used with a ball mass of 75 grams. The powder and milling balls occupied about 25% of the working volume of the cannister. Following the initial hour of mechanical alloying, the powder was sieved through a 100 μm screen to segregate the coarse fraction. The coarse fraction was milled for an additional ten minutes to reduce it to a finer powder, sieved to eliminate any residual coarse particles, and recombined with the original powder lot.

Table II

POWDER CHARACTERISTICS

	Tungsten	*Copper*	*Cobalt*
Supplier	GTE	University	Alfa
Size Range	1-10 μm	10-40 μm	10-40 μm
Principal Impurities (wt ppm)	C(10), O(740), Cu(500), Fe(200), Y(3600)	Pb(1600)	C(680), S(470), Cu(20), Fe(30), Ni(800)

Powders were cold compacted in a single action cylindrical die having a diameter of 13.0 mm. The compaction pressure was 335 MPa and no die lubricant was used. For all compositions, a cylindrical pellet was obtained which exhibited good green strength. The green density for all materials, regardless of powder mixing technique, was in the range of 56%-59% of theoretical.

Elevated temperature sintering was conducted in a dry hydrogen environment at temperatures in the range of 1083° C to 1430° C. The furnace chamber and specimen holder were constructed of high purity alumina. Temperature was monitored with a Type S (Pt-Pt/10% Rh) thermocouple placed in close proximity to the specimen being sintered. A positive-pressure gas delivery system was constructed for these experiments with input flow determined by calibrated flow meters and output flow insured through the use of twin bubblers. The rate of gas flow for all experiments was chosen so as to exchange the atmosphere in the furnace

volume once every ten minutes. This corresponded to a flow rate of 6.7×10^{-2} l/sec.

The moisture content of the process gasses was monitored with a thermoelectrically cooled optical dewpoint sensor. Dewpoint of the Ar gas used for system purging was -45° C and the dewpoint of the H_2 process gas was in the range of -35° C to -39° C. An apparatus was available to inject moisture into the process gas during sintering. Previous experiments with the W-Ni-Fe system have established that a high dewpoint can reduce porosity by suppressing condensation of gasses which are dissolved in the liquid during the solution-reprecipitation stage of liquid phase sintering [13]. In the W-Cu-Co system, however, there is only limited solubility of W by the Cu+Co liquid. Thus, gasses which may be present in solid solution within the W particles will not be released into the liquid by dissolution of the W. Early experiments in this program demonstrated that high dewpoints had no observable effect on the densification behavior in the W-Cu-Co system.

The general sintering method involved exposure to dry hydrogen at a low temperature to reduce surface oxides present on the elemental powders, followed by a high temperature sinter to consolidate the material. The low temperature reduction was performed at 800° C for a period of one hour. The heating rate up to the sintering temperature was 15 °C/min. The cooling rate from the sintering temperature to the matrix solidus temperature was 40 °C/min with a somewhat slower furnace cooling to room temperature. Except for purging of the furnace and gas lines prior to the start of the heating cycle and purging prior to specimen removal after complete cooling, the dry hydrogen atmosphere was used throughout the sintering cycle.

Sintering temperatures were chosen on the basis of the published Cu-Co equilibrium diagram [23]. As a simplifying assumption, the liquation temperature in the W-Cu-Co system was hypothesized to be independent of the presence of W. (This assumption is probably acceptable for the first liquid which forms, although subsequent analyses by X-ray diffractometry and Auger spectroscopy indicate that the composition of the matrix changes during sintering. This topic is discussed in greater detail below.) The

minimum sintering temperature was then chosen by determining the liquidus temperature for the particular Cu:Co ratio being used.

Following sintering, a number of analyses were conducted to characterize the sintering behavior in the W-Cu-Co system. The density was determined by carefully measuring the mass and volume of sintered specimens.

The hardness of the as-sintered materials was measured as well. Hardness measurements were conducted using the Rockwell R_A range because this range spans the full range of hardnesses encountered in the present work. Hardness measurement with a large indenter, such as that used in the Rockwell test, is preferred over microhardness techniques such as the Vickers or Knoop methods. Microhardness measurements do not measure the hardness over a sufficient volume of material and significant variation in readings may be expected. Hardness measurements were taken on lightly ground cross sections through the sintered cylinders after mounting in bakelite. Five readings were taken and the average value is presented.

Extensive microstructural characterization was also carried out on the as-sintered materials. Of particular importance in liquid phase sintering experiments is a determination of the dihedral angle. The dihedral angle provides an indication of the energy ratio between the W-W grain boundaries and the W-liquid surfaces [25,26]. This ratio is dependent upon the composition of the liquid in equilibrium with the W particles and thus, may be expected to change as the sintering parameters and composition are varied. Efforts were made to determine this angle for all materials sintered. High-magnification SEM photographs were taken and the dihedral angle measured directly from the photographs. Previous analyses indicate that the dihedral angle can be measured from two-dimensional photographs to within an accuracy of 5° [27]. For the present study, a sufficient number of photographs were taken so as to provide 20-30 angles which could be measured. For all cases, a calibrated grid was used to insure that no spherical aberration was occurring which might distort the image being recorded by the SEM. This experimental control was found to be quite valuable in insuring the collection of accurate information.

Additional microstructural characterization was conducted by SEM to determine the evolution of the microstructure with changing sintering

variables and also to determine the morphology of the elemental and mechanically alloyed powders. Optical metallography was conducted to provide an overview of the extent of porosity. Auger analyses and X-ray diffractometry scans were conducted to determine the solubility of W in the matrix phase during sintering and to determine the segregation of Co during sintering. Finally, a TEM investigation was conducted on a diffusion couple between liquid Cu+Co and a W substrate. This investigation provided insight into the phase relationships which may be established during liquid phase sintering in the W-Cu-Co system.

Results and Discussion

The results of our study of sintering behavior in the W-Cu-Co system have revealed two important mechanisms which lead to enhanced densification in this system: the effect of mechanical alloying and the effect of Co addition. Improved sintering conditions rely on both of these mechanisms. However, sufficient experiments were conducted to clearly distinguish the beneficial role of each of these effects separately. Mechanical alloying effects and the effect of Co addition are treated separately below.

Effect of Mechanical Alloying

When blended elemental powders of the 85W-15Cu composition were sintered at 1100° C for 1 hour, a relatively porous material was produced, with the density being only 60% of theoretical. At higher sintering temperatures, the density improved slightly, increasing to 67% of theoretical at 1430°C. This result indicates that densification by particle rearrangement upon liquation is not effective at yielding a highly dense material. When the elemental W and Cu powders are mixed through the action of mechanical alloying however, higher densities were obtained. At the highest sintering temperature examined - 1430°C - the mechanically alloyed 85W-15Cu powder sintered to a density of 74% of theoretical. A comparison of the densities for 85W-15Cu showing the effect of mechanical alloying is presented in Figure 10. The density of Co-containing compositions is also shown in Figure 10. The density of the mechanically alloyed material is consistently better than that of the conventionally blended powder. It is also seen that substantial variations in the sintering time for the 85W-15Cu or 85W-12Cu-3Co materials have little effect upon the final density

achieved. Similarly, for compositions containing Co, the density is improved through mechanical alloying. The density of a Co-con-taining composition is also shown in the comparative graph of Figure 10.

Density improvement via mechanical alloying can be explained by considering standard models for the initial stage of liquid phase sintering [16,17,25]. Upon liquation of the W-matrix mixture, it is to be expected that capillary forces draw the liquid into the small pores between individual W particles. When the liquid is drawn off in this fashion, a void is left behind at the original site of the matrix particle. Such a void is shown in Figure 11. Note that the void exhibits an irregular shape and that the walls of the void are ringed by a combination of matrix phase and tungsten particles. The void shown can only be filled by *rearrangement* of W particles or by *growth* of nearby tungsten particles. Due to a non-zero dihedral angle in the W-Cu-Co system, W-W particle contact can be extensive and result in the formation of a skeletal network of W particles. The formation of such a network inhibits densification by the *particle rearrangement* mechanism. Particle growth may fill the void directly or displace liquid back into the void as coarsening progresses. Densification by *particle growth* occurs very slowly in the W-Cu system because the primary mechanism of grain coarsening - solution/reprecipitation - is supressed by selection of the Cu matrix. Instead, W particles coarsen by neck growth and coalescence of neighboring grains at points of W-W particle contact. This coarsening process is controlled by sluggish solid-state diffusion processes. With prolonged sintering times, the pore assumes an equilibrium spherical shape as shown in Figure 12. Note that the boundary of this pore is a continuous ring of W grains. Such a pore structure is very stable because liquid cannot be displaced into the pore and gaseous species cannot diffuse out of the pore. Thus, longer sintering times are not expected to improve the density for the case of conventionally blended powders.

Preparation of powders by mechanical alloying provides a material which has a much finer degree of mixing than the conventionally blended materials. Examination of the powders indicated that 1 hr of mechanical alloying was sufficient to produce particles with a fine lamellar structure. An example of mechanically alloyed 85W-15Cu powder is presented

in Figure 13. Shown are lamella of W having a thickness of 1-2 μm separated by a thin film of Cu. True atomic-level alloying via mechanical alloying was not achieved in the W-Cu-Co system of this study. A recent review article by Koch discusses the issues affecting the amount of mixing which is attainable in immiscible systems such as W-Cu [28]. Detailed analyses of mechanical alloying of binary immiscible systems such as Al-Ge and Ge-Pb indicate that microstructural refinement reaches a limit when the effect of mixing is counterbalanced by the thermodynamics of the alloy system which requires a large positive heat of mixing. For the immiscible systems studied, this limit was reached when the individual components had a size of about 20 nm. Thus, the mechanical alloying of W-Cu mixtures for times in excess of 1 hr would doubtless produce greater microstructural refinement. This avenue of research is the subject of ongoing investigations.

By mechanically alloying the elemental powders, the size of the void which forms upon initial liquation is greatly reduced. Shown in Figure 14 is the 85W-15Cu specimen which was sintered from mechanically alloyed powder for 1 hr at 1183° C. As expected, the action of mechanical alloying has resulted in the formation of a plate morphology with alternating layers of W and matrix phase. The liquid-forming (matrix) phase is very finely dispersed prior to liquation and large voids of the type shown in Figs. 11 and 12 are not observed. As the matrix phase is drawn into the smallest pores between the W platelets by capillary action upon liquation, only a small void is left behind at the original site of the matrix particle.

Further, it is expected that the plate morphology of the mechanically alloyed W particles leads to a greater degree of rearrangement when liquation occurs than the quasi-spherical W particles. Shrinkage during the rearrangement stage of liquid phase sintering is driven by attractive forces between adjacent particles which are bridged by a wetting liquid. Theoretical analyses for rearrangement of *spherical* particles predict that the rearrangement forces are greatest as the particle size decreases, as the interparticle distance decreases, as the degree of wetting by the liquid increases, and as the volume of liquid decreases [18,30]. These predictions have been confirmed by a number of researchers [31,32]. More recently, a theoretical treatment has been provided for the rearrangement

forces associated with *irregularly-shaped* particles [33]. Attractive forces between irregularly-shaped particles bridged by a wetting liquid differ in several respects from the forces which operate between spherical particles. Most importantly, neighboring irregularly-shaped particles may experience normal, shear, or torsion forces - depending upon the contact geometry of the neighboring particles. By contrast, spherical particles can only experience normal attractive forces. Thus, it is predicted that there is a greater driving force for rearrangement with irregularly-shaped particles. As a result, voids observed in materials sintered from mechanically alloyed powder are finely divided, fewer in number, and exhibit the same size scale as the W particles. Typically, voids observed in powder prepared by mechanical alloying are entirely surrounded by the matrix phase. Such a void is shown in Figure 15.

The plate morphology produced by mechanical alloying leads to an interesting evolution of the microstructure as sintering proceeds. As shown in Figure 14, the initial microstructure consists of colonies of plates representing the alternating W and matrix layers of the mechanically alloyed powder. The dimensions of the plates are somewhat smaller in size than the initial powder. Such a platelet structure does not represent an equilibrium microstructure for the W-Cu or W-Cu-Co system. As sintering proceeds, the W plates tend to spheroidize. Shown in Figure 15 is an example of a spheroidized microstructure. It was found that Co addition plays a central role in promoting spheroidization. Thus, a discussion of this phenomenon is presented in the following section.

A comparison of hardness between conventionally blended and mechanically alloyed materials is presented in Figure 16. For liquid phase sintered materials in general, hardness is expected to reflect porosity fraction, extent of particle contiguity†, strength of the individual matrix and particle constituents, and particle coarsening. Lee and Gurland have proposed a microstructural model to account for the contribution of each of these factors [29]. They use a rule-of-mixtures approach based upon the Hall-Petch formula to provide a quantitative prediction of the hardness. Thus, hardness measurements can provide valuable information on

† *Contiguity* is a measure of the amount of contact area between solid particles in liquid phase sintered materials.

microstructural features which density measurements alone cannot address. For the 85W-15Cu composition, mechanical alloying results in a nearly twofold increase in hardness. This is attributable to the decrease in porosity obtained by mechanical alloying. There is an additional twofold increase in the hardness of the 85W-15Cu material when the highest sintering temperature is used. The hardness increase brought about by the use of a higher sintering temperature may be attributed to greater contiguity of the W particles as well as improved density. Higher sintering temperatures lead to increased levels of W transport via solid state diffusion. This results in accelerated neck growth and grain coalescence at W-W particle contact points. For the Co-containing composition, there is also a significant hardness increase for the mechanically alloyed material as compared to the conventionally blended material. This hardness increase is associated with the density increase, previously shown in Figure 10. A slight hardness increase is shown for longer sintering times with the 85W-12Cu-3Co composition. This hardness increase may be attributable to a greater degree of W-W particle contiguity associated with longer sintering times.

Effect of Co Addition

The effect of Co addition on the sintering characteristics of the W-Cu-Co system was to increase both the density and hardness of the sintered product. This was seen most clearly for the case of the mechanically alloyed materials in which the combination of Co addition and mechanical alloying led to densities in excess of 90% of theoretical. A plot of density as a function of Co content for selected W-Cu-Co compositions is shown in Figure 17. The addition of 1% Co leads to a significant increase in density over the binary W-Cu material. A further increase in Co to the 3% level has only a slight beneficial effect on the density.

Hardness data for the three mechanically alloyed compositions are presented in Figure 18. The hardness of the W-Cu and W-Cu-Co materials is seen to increase with longer sintering times and increased sintering temperatures. As discussed in the previous section, hardness variation in liquid phase sintered materials may be attributable to a number of factors. The hardness variability presented in Figure 18 may be attributable to

either a Co-related strengthening effect, improved density, or to increased contiguity. To further explore this area, a microstructural investigation was conducted on the as-sintered materials.

Since the mechanically alloyed materials exhibited the best density, a discussion of microstructural evolution during sintering will be limited to these materials. When the tungsten and matrix powders are mixed by mechanical alloying, particles are formed which exhibit a lamellar structure, Figure 13. The lamella consist primarily of tungsten plates separated by a thin film of the matrix material. Upon heating to the sintering temperature, a process of spheroidization begins. Spheroidization is initially driven by the excessive strain energy in the heavily cold-worked tungsten platelets which causes them to recrystallize. Recrystallization is followed by the establishment of an equilibrium dihedral angle between the solid grains and the liquid matrix. Additional sintering time results in grain growth. The spheroidization observed never reaches completion - discrete spherical particles do not form.

Generally, spheroidization of lamellar structures may be explained in terms of a grain boundary grooving theory or a fault boundary migration theory. Although a rigorous analysis of the spheroidization phenomenon has not been conducted, the observed behavior appears to fit the grain boundary grooving model proposed by Mullins [34]. Spheroidization of platelet structures via fault boundary migration requires transport between adjacent platelets, presumably through the liquid phase [35]. The slow rate of spheroidization and grain coarsening in the experiments of this study suggest that liquid phase transport of W between neighboring W particles is not a dominant mechanism, however. Further definition of the mechanism of spheroidization in the W-Cu-Co system would require an extensive study of the kinetics of microstructural evolution and has not being actively pursued.

The microstructures of the 85W-15Cu, 85W-14Cu-1Co and 85W-12Cu-3Co materials are shown in Figures 19, 20, and 21, respectively. The three materials shown in Figures 19-21 were sintered under identical conditions: 1430° C for 1 hr. The effect of Co content on the W platelet spheroidization is readily observed. When no cobalt is added, Figure 19, spheroid-

ization of the tungsten platelets is incomplete. The W platelets have fully recrystallized but are still recognizable as discrete platelet colonies. The addition of 1% Co, Figure 20, leads to a sintered microstructure with a greater degree of W spheroidization. Cobalt addition also leads to grain growth. The addition of 3% Co leads to additional grain growth and a similar degree of spheroidization as compared to the case of 1% Co addition. The transformation of the microstructures shown in Figures 19-21 from the mechanically alloyed lamellar morphology involves a number of processes which require transport of W. The observed grain growth may result from coalescence of adjoining W grains. Coalescence occurs by boundary migration and is known to be controlled by bulk diffusion or grain boundary diffusion processes [36]. Grain boundary grooving to establish an equilibrium dihedral angle is likewise dependent upon diffusion processes within and among the W grains [34]. The materials shown in Figures 19-21 were designed to be sintered at a common temperature in order to establish experimental conditions of invariant solid-state W diffusivity among each of the compositions studied. Thus, the microstructural variation shown in the above figures can only be attributable to the effect of Co on the transport of W during sintering. Possible effects include Co-related surface activation similar to the activate solid-state sintering phenonemon or an increase in the level of W solubility in the matrix phase due to the Co addition.

The extent of time and temperature during sintering were also found to influence the degree of microstructural transformation of the mechanically alloyed materials. Shown in Figure 22 is the 85W-14Cu-1Co composition sintered at 1280° C (100° C in excess of the Cu+Co liquidus temperature) for 1 hr. The microstructure of Figure 22 exhibits only a limited degree of spheroidization and the prior platelet colonies may still be discerned. As shown previously, Figure 20, this composition exhibits a greater degree of grain growth and spheroidization when sintered at 1430° C. This difference may be explained by the enhanced rate of W diffusion at the elevated sintering temperature.

It is also to be observed in Figures 19-22 that the pore size and distribution for mechanically alloyed materials differ greatly from the powders prepared by conventional mixing. It was previously shown, Figures

11 and 12, that conventional mixing of powders results in the formation of large and stable pores which occupy a volume ten or more times greater than the grain volume of the heavy alloy. Powder preparation by mechanical alloying not only reduces the overall volume fraction of pores - as indicated by improvements in density - but leads to the creation of pores which are of the same size as the W grains. Furthermore, all pores prepared from mechanically alloyed powders are largely surrounded by the matrix phase.

In order to more quantitatively describe the degree of spheroidization observed for the microstructures of Figures 20-21, measurements of the dihedral angle, ϕ, were made. (Due to a limited degree of spheroidization and a higher volume fraction of pores, the dihedral angle for the non-Co composition could not be accurately determined.) The dihedral angle provides a measure of the extent of liquid intrusion among adjoining W grains and also provides a measure of the ratio of solid-solid surface energy to solid-liquid surface energy, γ_{ss}/γ_{sl}. The surface energy ratio, γ_{ss}/γ_{sl}, may be derived from measurements of the dihedral angle ϕ through use of the Young Equation [27]:

$$2\gamma_{sl}\cos\left(\frac{\phi}{2}\right)=\gamma_{ss}$$

Measurements of ϕ indicate a strong dependence on the amount of Co addition and a somewhat weaker dependence on the sintering conditions. The measured values of the dihedral angle are presented in Table III together with the calculated ratio of γ_{ss}/γ_{sl}.

Table III

MEASURED VALUES OF THE DIHEDRAL ANGLE, ϕ, AND CALCULATED VALUES OF THE SURFACE ENERGY RATIO

Composition (wt %)	Sintering Conditions	ϕ	γ_{ss}/γ_{sl}
85W-14Cu-1Co	1 hr, 1280° C	88°	1.44
85W-14Cu-1Co	3 hr, 1280° C	87°	1.45
85W-14Cu-1Co	1 hr, 1430° C	83°	1.50
85W-12Cu-3Co	1 hr, 1430° C	66°	1.68
85W-12Cu-3Co	3 hr, 1430° C	64°	1.70

Assuming that the solid-solid surface energy is constant among all experiments (if the composition of the W grains is constant in all experiments), the change in the surface energy ratio may be attributed to a decrease in the liquid-solid surface energy with Co addition. The Young Equation predicts that the surface energy ratio approaches a limiting value of 2 as the dihedral angle approaches 0°. This condition would indicate complete liquid penetration of the W-W grain boundaries. It is generally recognized that lower values of the solid-liquid surface energy and a low dihedral angle are favorable for enhanced densification during liquid phase sintering. The data of Table III indicate that Co addition and sintering parameters affect the surface energy and dihedral angle.

To assess the role of Co in the W-Cu-Co system, as-sintered specimens were examined by X-ray diffractometry and Auger spectroscopy. X-ray diffractometry scans were conducted on polished cross sections of the as-sintered materials using Cr Kα radiation at an operating potential of 35 kV. The Auger analyses were conducted at an operating voltage of 5 kV on polished cross sections. Additionally, transmission electron microscopy was used to examine phase relationships in the W-Cu-Co system. For the TEM study, the specimen consisted of a Cu+Co liquid deposited onto a W substrate as part of an earlier investigation into wetting phenomenon [37].

The X-ray diffraction study indicated that both the 85W-14Cu-1Co and 85W-12Cu-3Co compositions which were sintered at 1430° C for 1 hr exhibited diffraction peaks for bcc W, fcc Cu, and the rhombohedral intermetallic phase W_6Co_7. No evidence was found for Co-rich precipitates in the Cu matrix. Auger analyses of the same specimens, however, found some evidence of Co in the matrix phase. Electron microscopy of the planar specimen revealed the presence of fcc Co precipitates in a Cu-rich matrix with a virtually identical lattice parameter to fcc Cu. Shown in Figure 23 is an example of Co precipitates in the Cu matrix. This TEM finding confirms earlier reports on the nature of precipitates in the Cu-Co binary system [38]. Apparently, the concentration of this Co-rich phase was too low to be detected by X-ray diffraction for the as-sintered specimens. The TEM study also showed that Co preferentially segregates to the W surface and forms the intermetallic compound W_6Co_7. An example of the rhombohedral

W_6Co_7 formed on a W surface is shown in Figure 24. Examination of Co-X binary phase diagrams suggest that Co is also soluble in Cu and W to a limited extent. Thus, the Co may be partitioned among Co-rich precipitates in the Cu matrix, the intermetallic compound W_6Co_7 at the surface of the W grains, or in dilute solid solution with the W grains or the Cu matrix.

Although a microchemical analysis of this complex system is far from complete, it appears that the Co preferentially segregates to the W particles during liquid phase sintering and forms the intermetallic compound W_6Co_7. Thus, the dihedral angles measured for the W-Cu-Co compositions, Table III, describe the equilibrium surface energy ratio between a W_6Co_7 layer and a Cu-Co liquid. The Co content of the liquid phase is different for each of the materials examined. This explains the difference in the experimentally determined surface energy ratios. Further, since the formation of the intermetallic W_6Co_7 phase depletes the liquid of Co, it is difficult to judge how much Co remains in the matrix phase. The amount of W_6Co_7 formed depends upon the available W surface area. Thus, the size of the W grains may play a role in determining how much W_6Co_7 forms. Similarly, the thickness of the W_6Co_7 layer may depend upon the sintering parameters of time and temperature.

The observation that the intermetallic W_6Co_7 compound forms is consistent with the previous work of Prill et.al. [39]. Their study showed that the solid-state sintering of W could be enhanced through the use of Co as an activator. Higher densities were obtained up to the Co concentration which was sufficient to form a monolayer on the surfaces of the W particles. Further increases in the amount of Co addition led to the formation of the intermetallic phase W_6Co_7 and no further improvement in the sintering was observed. Prill et al concluded that the diffusion of W through the intermetallic layer would be slow and thus, further transport of W in this system would be retarded. The present system is more complex than that studied by Prill et. al. because Co may be distributed among four different phases. In the present study, the intermetallic W_6Co_7 phase was observed for both Co-containing compositions examined. Absorption of Co at the W surface provided the beneficial effect of improving the wetting characteristics of the liquid matrix. Improved wetting, in turn, enhances rearrangement processes and results in improved density. The improved

wetting provided by Co addition is the principal reason for the enhanced sintering characteristics of the Co-containing compositions relative to the binary W-Cu composition.

As previously noted, however, the microstructural evolution of the sintered materials suggests that Co addition plays a role in enhancing the transport of W. The partial spheroidization of the mechanically alloyed W platelets and coarsening of W grains were shown to depend upon the level of Co addition. Grain growth requires W transport as does the formation of an equilibrium dihedral angle. Possible transport schemes include solid state diffusion at points of W-W particle contact (coalescence), transport through the liquid (solution/reprecipitation), and surface diffusion at the W-matrix boundary. Auger analysis of the matrix phase indicates that W is present in the matrix for the 85W-12Cu-3Co composition but is not present in the matrix of the 85W-14Cu-1Co composition. The amount of W measured in the matrix of the 85W-12Cu-3Co was 7 atomic percent (14 weight percent) with a potential error of ±5 atomic percent. The error is large because the amount of W detected was only slightly above the noise level of the continuous Auger spectrum. Due to the large error involved, such a measurement cannot be regarded as conclusive. The Auger analysis suggests that increased Co addition leads to increased solubility of W in the matrix phase but does not provide a firm quantitative result. Overall, grain coarsening in the W-Cu-Co system is very sluggish. While liquid phase transport of W may play a role in microstructural evolution for the higher Co contents, the slow rate of particle coarsening suggests that the liquid-phase transport of W plays only a minor role. The precise nature of W transport in these materials requires further study.

Summary of Sintering Behavior in the W-Cu-Co System

The previous sections have described experiments which explored sintering parameters and compositional variations. We described the full range of phenomenon observed in terms of density, hardness, and microstructural evolution. What has emerged is a picture of liquid phase sintering which is quite different than the traditional three-stage process of which the W-Ni-Fe and W-Ni-Cu systems are typical.

The initial stage of liquid phase sintering in the W-Cu-Co system involves liquation of the matrix phase and initial densification by particle rearrangement. As with all liquid phase sintering systems, capillary forces draw off the liquid into the smallest pores between the solid particles resulting in the formation of a void at the original site of the matrix particle. The importance of mechanical alloying is to reduce this effect by greatly refining the initial matrix particle size and also by reducing the size of pores among the W particles into which the liquid may be drawn. The importance of Co addition is to improve the wetting characteristics of the liquid through preferential segregation of the Co to the W surfaces and formation of the intermetallic compound W_6Co_7. For the mass fractions of W studied - 85% - a great degree of W-W particle contact was observed. This effect is due to both the high fraction of W used as well as the relatively high values of the dihedral angle which prevent complete liquid intrusion among the W grains. The effect of such extensive W-W contact is that a solid skeleton of W is formed early in the sintering process and this skeleton inhibits densification by the particle rearrangement mechanism. Particle rearrangement can be more effective for mechanically alloyed powders, however, because the mechanically alloyed tungsten platelets will experience a greater driving force for rearrangement than non-mechanically alloyed W spheres.

A second stage of sintering in the mechanically alloyed W-Cu-Co system involves the increased densification brought about by W spheroidization and W grain growth. Mechanical alloying, in addition to reducing the size of the initial pores formed upon liquation, provides a microstructure which may exhibit a morphological evolution by the spheroidization of the W platelets. This is initiated by recrystallization of heavily cold worked W platelets and partially driven by the energy requirement for an equilibrium dihedral angle at all W-W-Matrix junctions. It has been shown in the present study that Co addition changes the liquid-solid interfacial energy and leads to greater spheroidization. Also observed was greater grain growth associated with Co addition. The precise nature of W transport during this stage has not been determined. Auger analysis suggests that W may be soluble to a limited extent in the Cu-Co matrix, but the amount of W detected was near the resolution of the Auger spectroscopic technique.

The sluggishness of grain growth during the sintering experiments of this study indicate that solution/reprecipitation is not a predominant mechanism of W transport. Rather, the Co-activated surface transport seen previously in solid-state activated sintering of W-Co materials may be more important.

Since the second stage of sintering in the W-Cu-Co system is driven by diffusional processes among the W grains, microstructural evolution is necessarily slow. This is because the sintering temperatures used are at a low homologous temperature with respect to the W, and bulk and surface diffusion processes are therefore expected to be sluggish. In all powder-processed material, final densification is achieved through grain growth which eliminates the residual porosity. Since grain growth occurs only very slowly in the W-Cu-Co system, complete densification by liquid phase sintering is probably not possible. Thus, while the primary goal of producing a heavy alloy with a fine grain size has been achieved, the attainment of full theoretical density in the W-Cu-Co system has not been achieved. The synthesis of a fully dense material would require additional processing such as HIP or hot pressing.

The W-Cu-Co system was chosen for study in order to obtain a heavy alloy which exhibits limited grain growth. This goal was accomplished. Factors affecting densification include method of powder blending and amount of Co addition. Optimum hardness and density are found when elemental powders of composition 85W-12Cu-3Co were prepared by mechanical alloying and sintered 100° C in excess of the Cu-Co liquidus temperature. The observed sintering mechanism differs from that of traditional liquid phase sintering in that particle coarsening via solution/reprecipitation is not a dominant densification mechanism. While favorable for maintaining fine grain size, the lack of a solution/reprecipitation mechanism inhibited the full densification of sintered materials in the W-Cu-Co system.

Task IIB: Consolidation of Tungsten via Solid State Sintering

The powder shown in Figure 9 was used for this task. The temperatures required for the sintering of W powders are in excess of 2000° C and require either electrical resistance heating or radiation heating using an ultra-high temperature furnace. These requirements were beyond the current capabilities of existing equipment at Lockheed.

Consequently, trial sintering experiments were conducted at Phillips Elmet, Lewiston ME. Two specimens of W-1.4% Y_2O_3 were cold compacted into 13 mm diameter cylinders and sintered at 1900° C for 3.5 hrs and 7 hrs, respectively. The results of these sintering trials are shown in Figures 25 and 26. Both specimens exhibited a significant level of porosity, although the specimen sintered for 7 hours has a reduced level of porosity. These microstructures are similar to that shown previously for the sintered W-2%ThO_2, Figure 1. As expected, a greater degree of grain growth is observed for the longer sintering time, Figure 26. Evidently, the Y_2O_3 dispersion has little effect on grain growth. It is evident that a fully dense material can be prepared from the W-Y_2O_3 powder only by sintering for longer times or higher temperatures or by mechanically working the sintered product. The former procedure would result in a greater degree of grain growth while the latter procedure would produce a non-equiaxed grain morphology. Both of these results are incompatible with the program objective: to produce a fine grained material. Thus, this task encountered the same problem as Task IA and was suspended. However, the result of this task and Task IA demonstrate the necessity for pursuing alternative means of obtaining fine-structure tungsten.

Task IIC: Fine Structure through use of Ultrafine (Nanometer) Powder

Pure tungsten powders having four different sizes ranging from 0.02 μm (20 nm) to 150 μm were procured for this study. Representative SEM micrographs of these powders are shown in Figures 27-30 for the 150 μm powder, 74 μm powder, 0.5 μm powder, and 0.02 μm powder, respectively. The original goal was to consolidate these powders to full density via liquid phase sintering using Cu+Co as the liquid sintering agent. The processing knowledge gained under Task IIA was used in this task and, so far, only a limited number of experiments have been conducted.

It is anticipated that a heavy metal alloy produced from the 0.02 μm powder may exhibit unusual properties. This powder was obtained from Sumitomo Metal Mining Ltd. of Japan. A TEM micrograph of the 0.02 μm powder is shown in Figure 30. Because of the ultrafine particle size, and thus its large surface area, the 0.02 μm powder has a reported oxygen

content of 2.0%. Consolidation of the ultrafine tungsten powder requires successful hydrogen reduction of this surface oxide during sintering.

Only two experiments were conducted under this task. Both 0.5 μm and 0.02 μm powders were combined with the Cu and Co powders via mechanical alloying. In both cases, the compositions prepared were 85W-12Cu-3Co and the sintering was conducted at 1430°C for 1 hr. The mechanical alloying conditions and sintering technique were identical to those described under Task IIA.

Photomicrographs of the as-sintered microstructures are shown in Figures 31 and 32 for the 0.5 μm and 0.02 μm powders, respectively. Unexpectedly, the powders coarsened to a size range of approximately 5 μm. The as-sintered density for both materials was 91% - similar to the values that were obtained previously for coarser powders. It is a well known effect that smaller diameter powders have a higher driving force for coarsening than larger diameter powders. This effect can be exploited by allowing sintering of fine powders at lower temperatures than coarse powders. In the present case, sintering procedures derived for use with coarser powders led to excessive grain growth. Although grain growth was relatively substantial for the two materials shown in Figures 31 and 32, the tungsten-based materials produced exhibited fine equiaxed grains in the size range of 5 μm. Such a material has not previously been available. Further optimization of the sintering parameters for these unique submicron powders could lead to additional improvements.

4.0 Summary

The goal of this program was to explore methods of producing fine-structure tungsten-based materials. Following an extensive survey of processing technology, six methods were selected for evaluation. The results of this evaluation are as follows:

- Processing of commercially available thoriated tungsten to obtain a fine, equiaxed grain size with a fine dispersoid distribution does not appear to be feasible. Full densification requires thermomechanical processing after sintering. Thermomechanical processing of this material results in dispersoid coarsening and the formation of anisotropic tungsten grains.
- Production of a fine two-phase microstructure appears to be feasible in the W-Cr system. Arc cast buttons of the composition W-4% Cr were produced and shown to contain a significant volume of Cr-rich particles. Such particles could be precipitated out during a thermomechanical processing treatment and result in a fine-structure tungsten-based material.
- It is possible to obtain fine-structure W sheet via chemical vapor deposition. Processing must be controlled to inhibit formation of a columnar grain morphology.
- Consolidation of W by liquid phase sintering using a Cu+Co liquid has been investigated. It was found that a combination of mechanical alloying and Co addition led to a material with a density in excess of 90% of theoretical. Most importantly, the material exhibited a sluggish grain growth rate. Thus, it was possible to produce a W-based material with a fine, 10 μm diameter, equiaxed grain size.
- Consolidation of W containing a dispersion of yttria was not successful in yielding a fully dense fine-structure material. Full densification would require additional thermal or mechanical processing treatments which would yield a material with an undesirable microstructure.

- The use of ultrafine W powders led to the production of a fine-structure tungsten material. Although only a limited number of experiments were conducted under this task, a W-based material with a fine, 5 μm diameter, equiaxed grain size was produced. Further experimentation could yield a material with an even finer structure.

The above four tasks which showed promising results could be used in future programs to produce quantities of fine-structure tungsten sufficient for characterization in tensile tests or ballistic tests. Within the scope of this one-year program, however, resources to conduct such a testing program were not available.

ACKNOWLEDGEMENTS

A number of scientists provided valuable assistance to this research program during the past year and their assistance is gratefully acknowledged. The W-Cr alloys were prepared with the assistance of Dr. Bob Svedburg at Westinghouse, solid state sintering experiments were conducted with the assistance of Mr. Mike Kim at Phillips Elmet, and Drs. Randich and Landingham at LLNL furnished CVD tungsten for our evaluation. The assistance of Dr. Debra Yaney in providing TEM analysis is also acknowledged.

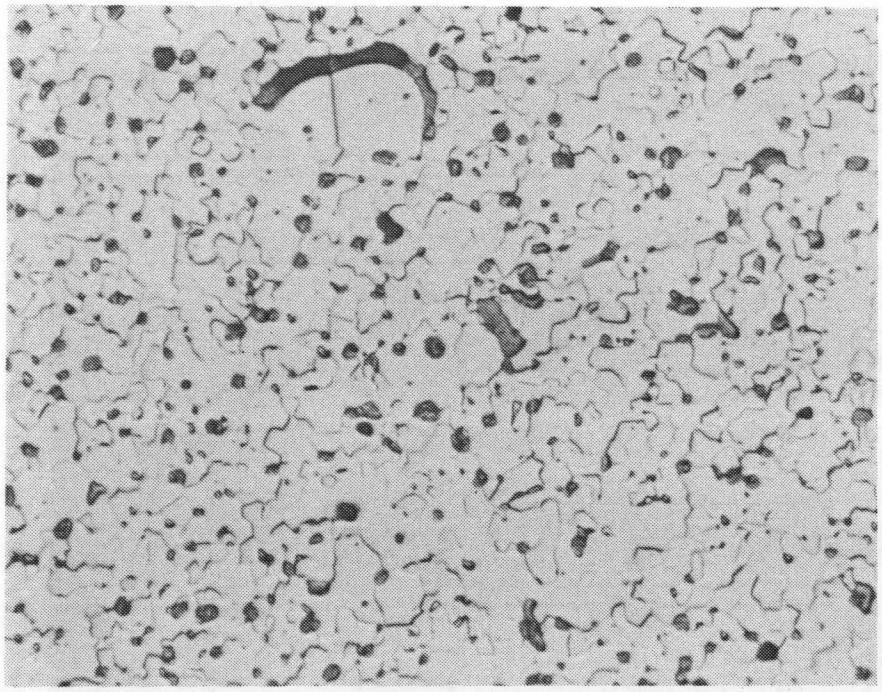

Figure 1
As-sintered W+2% Thoria. Sintered density is 90%. Tungsten grains and thoria particles are fine and equiaxed.

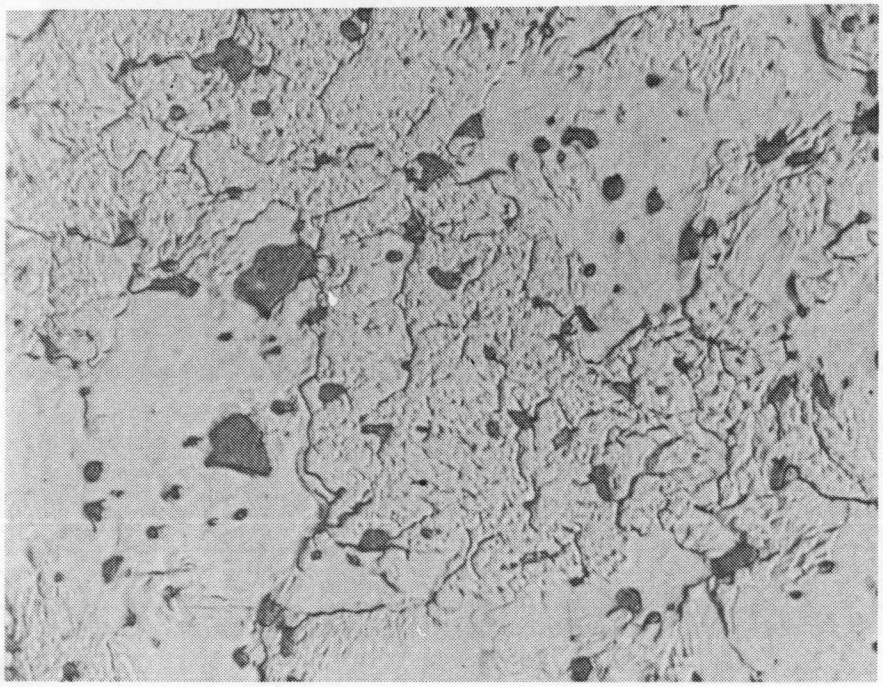

Figure 2
Transverse cross section from 30 mm diameter thoriated-W bar. Thoria particles (dark) are coarse and W grains have a size in the range of 50 µm.

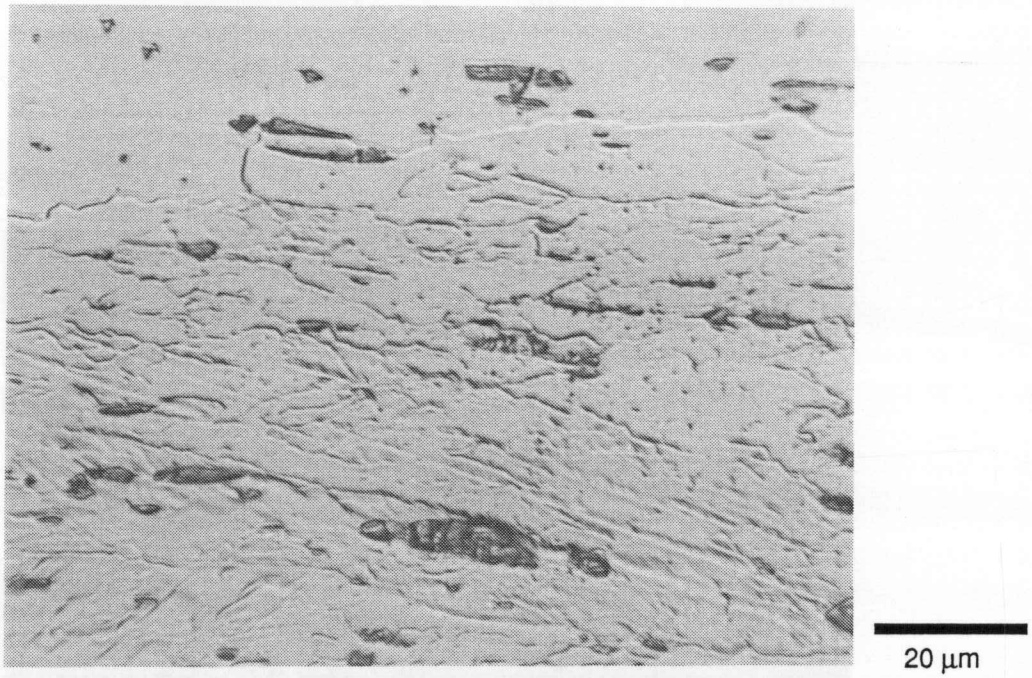

Figure 3
Longitudinal cross section from 30 mm diameter thoriated-W bar. Thoria particles and W grains are elongated due to unidirectional processing.

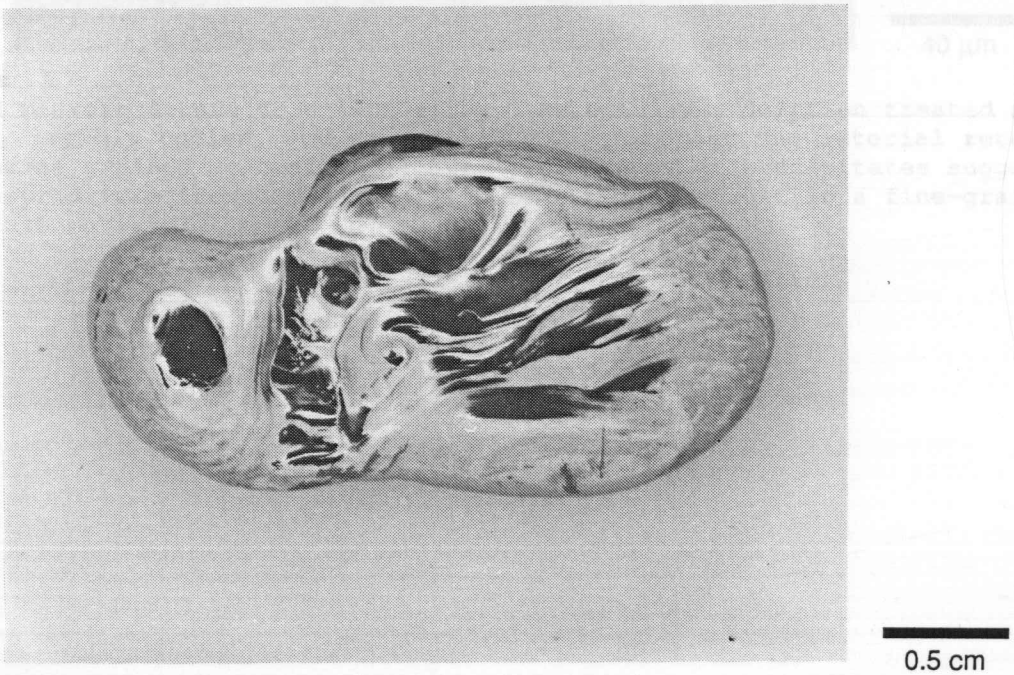

Figure 4
Arc melted button prepared from pure W rod. Though melting was successful, insufficient cooling of the copper hearth led to local copper melting and contamination of the W button.

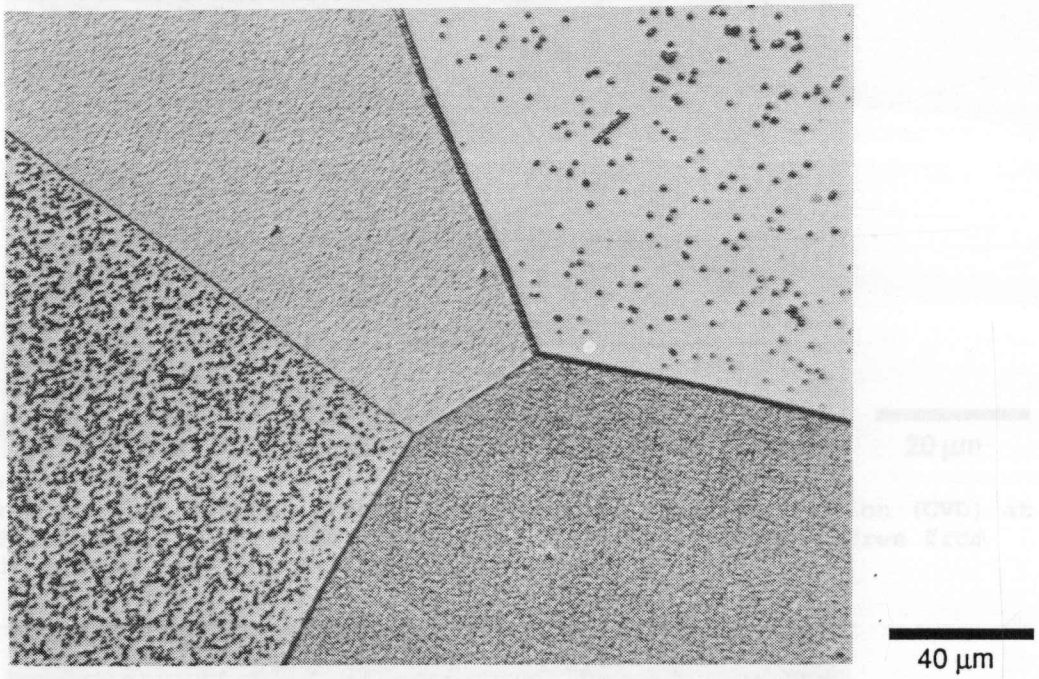

Figure 5
Etched microstructure of W-4%Cr alloy. Material was Solution treated at 1400°C, rapidly cooled, and aged at 1000°C. Although the material retains the coarse grained as-cast structure, presence of Cr precipitates suggest that appropriate thermomechanical treatment could result in a fine-grained two-phase material.

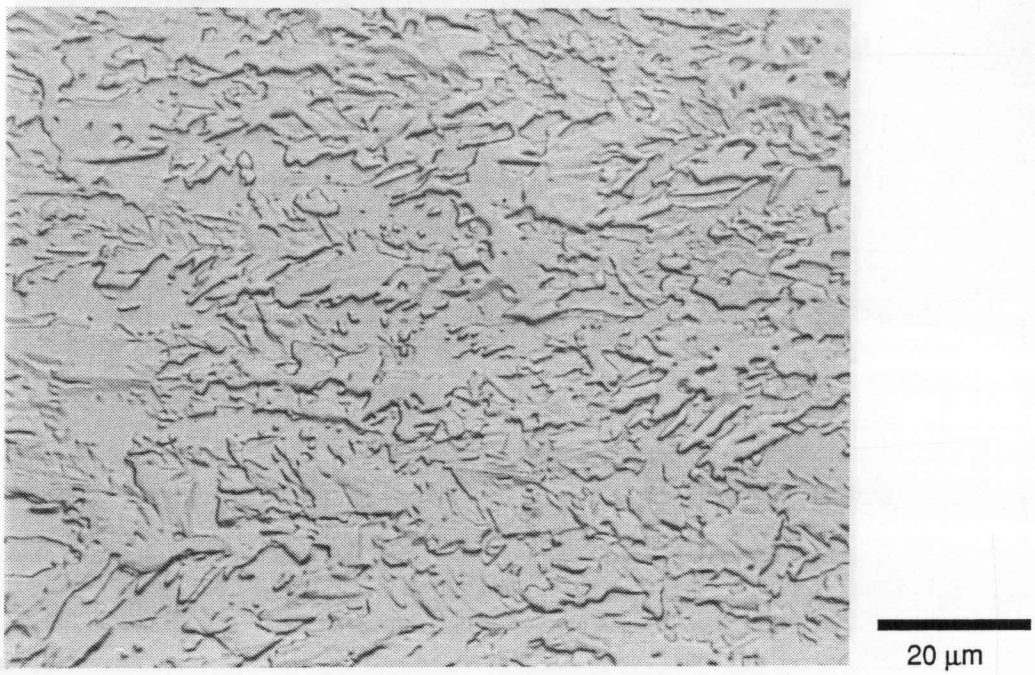

Figure 6
Microstructure of W sheet prepared by chemical vapor deposition (CVD) at COMURHEX (France). The material appears to be fully dense, free from inclusions, and exhibits a slight growth texture.

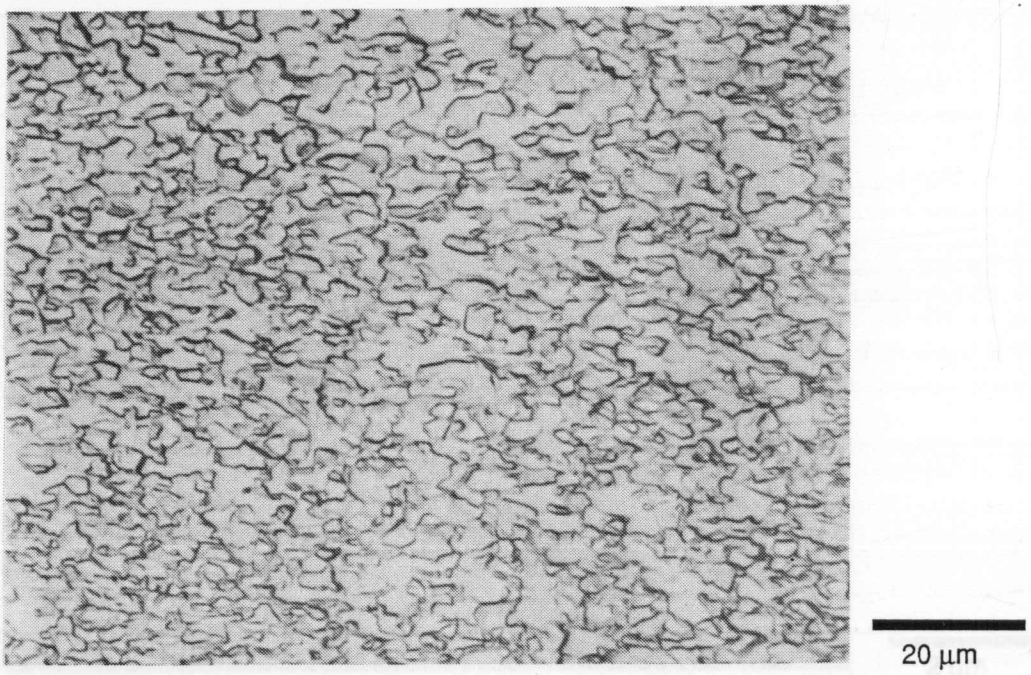

Figure 7
Microstructure of CVD W cylindrical shell prepared by LLNL. Grain size is finer than the COMURHEX material but grains retain a 2:1 aspect ratio due to growth texture.

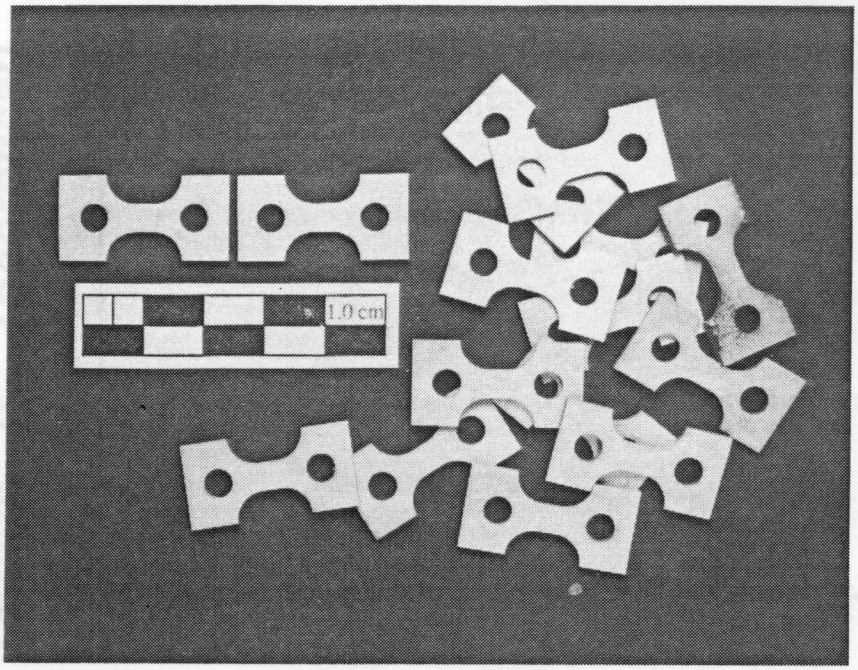

Figure 8
Tensile coupons prepared by electro-discharge machining from CVD-tungsten sheet. Prior to testing, specimens were lapped and electrochemically polished to insure a defect-free surface finish.

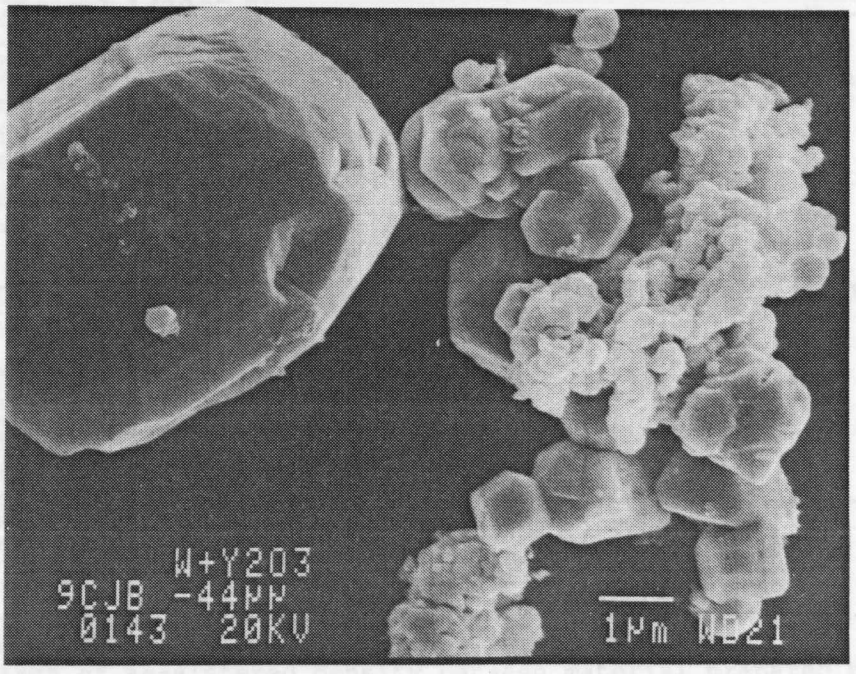

Figure 9
SEM micrograph of W+1.4% (vol) Y_2O_3 powder. Powder is reported by the supplier to have a mean particle size of 4.5 µm.

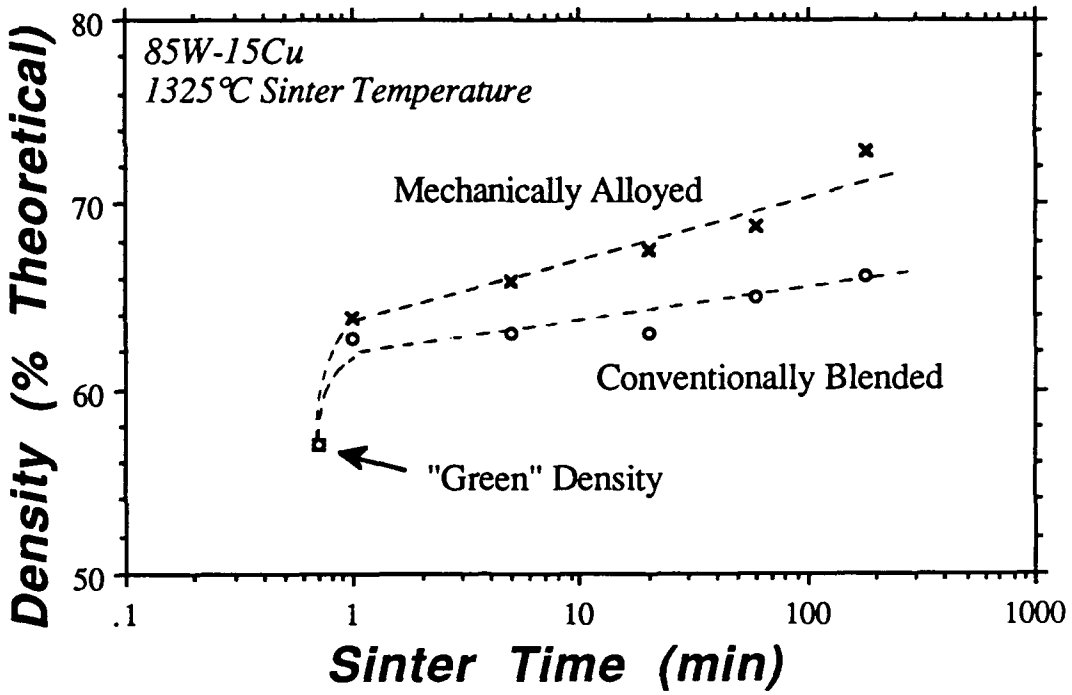

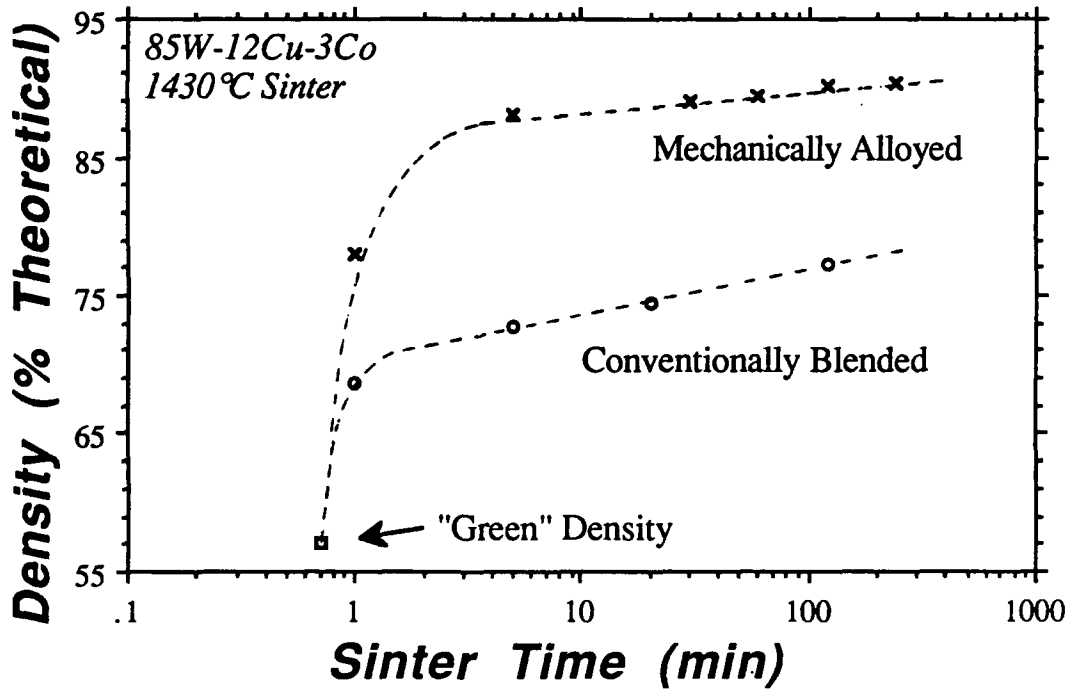

Figure 10
Comparison of as-sintered density between material prepared by conventional blending of powders and material prepared by mechanical alloying of powders. Materials prepared by mechanical alloying are consistently denser.

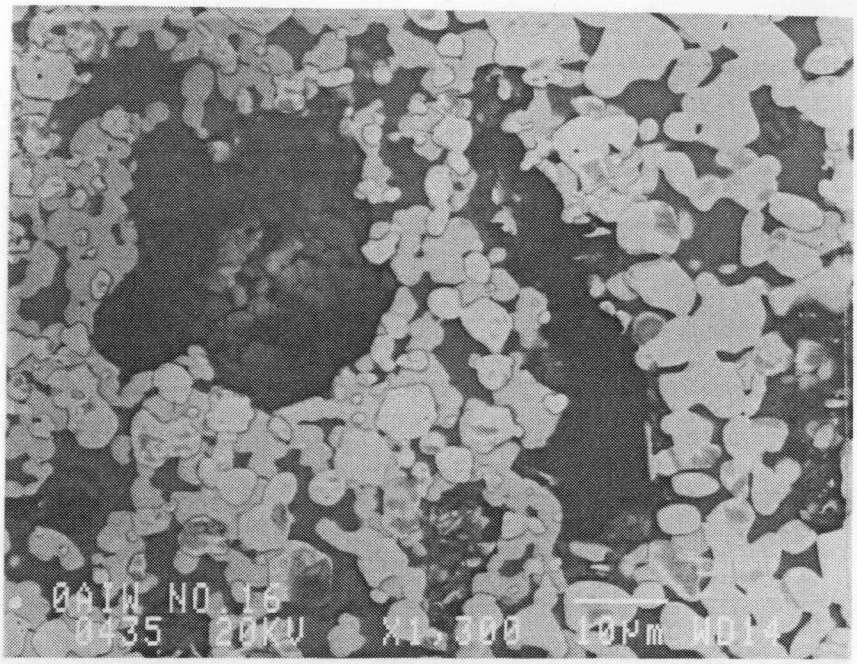

Figure 11
85W-12Cu-3Co sintered 1 hr at 1430° C, powder prepared by conventional blending. Shown are two typical pores with volumes many times greater than the W particle size.

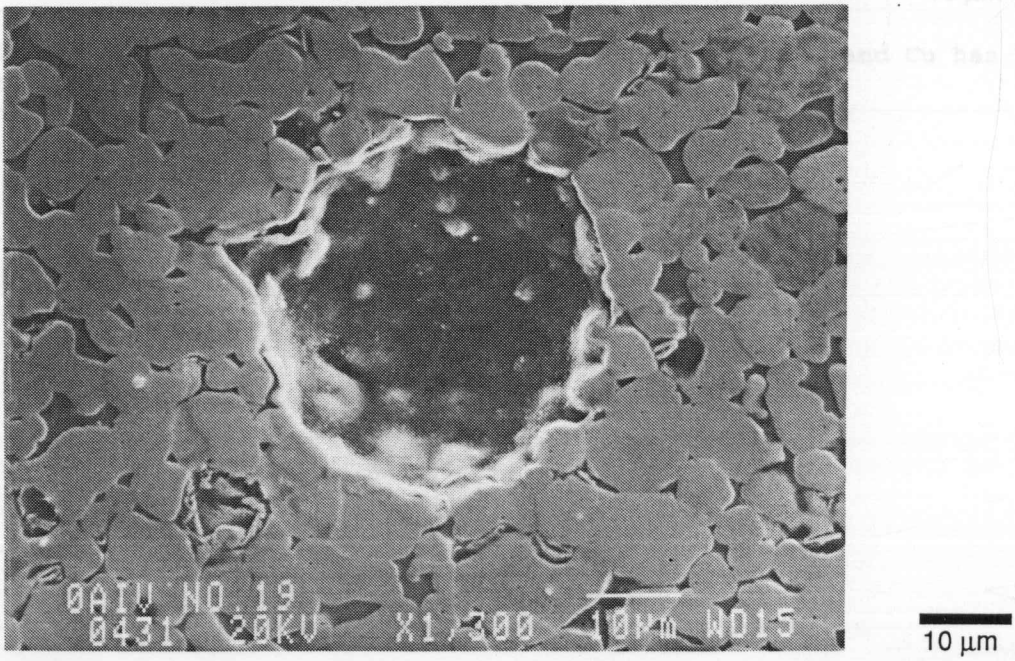

Figure 12
85W-12Cu-3Co sintered 3 hr at 1430° C, powder prepared by conventional blending. Prolonged sintering results in large spherical voids. Void is very stable because the perimeter consists entirely of W grains.

Figure 13
Mechanically alloyed 85W-15Cu powder. Intimate mixing of W and Cu has been achieved by 1 hr of mechanical alloying.

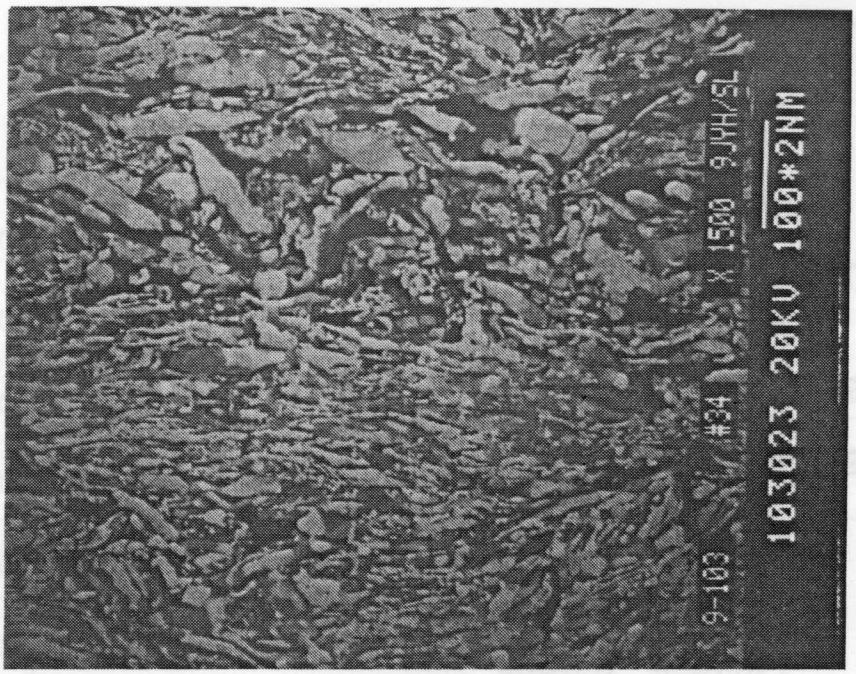

Figure 14
85W-15Cu, prepared by mechanical alloying, sintered 1 hr at 1183° C. Matrix and W powders are finely blended by mechanical alloying and no large voids are observed.

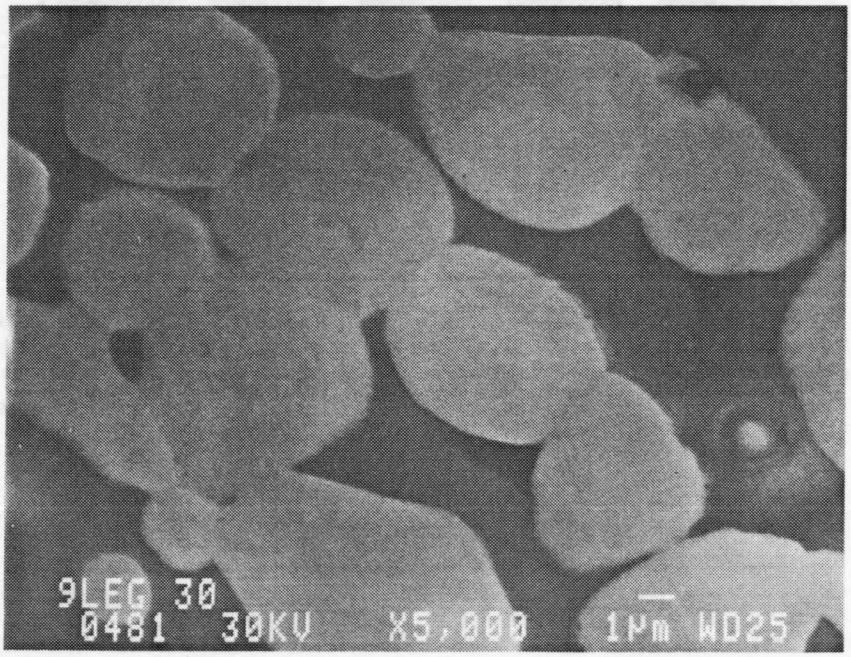

Figure 15
85W-12Cu-3Co, prepared by mechanical alloying, sintered 3 hr at 1430° C. Voids are of the same size as the W particles and are mostly surrounded by the matrix phase.

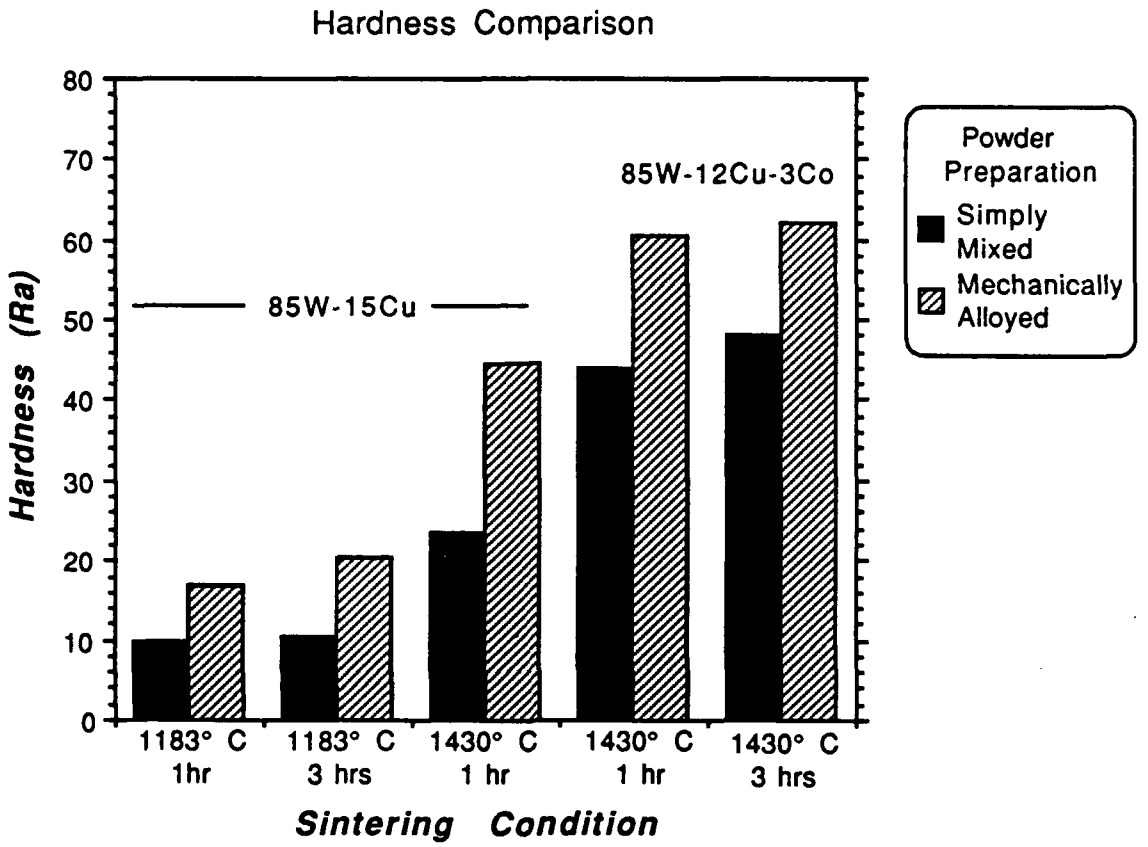

Figure 16
Comparison of as-sintered hardness between material prepared by conventional blending of powders and material prepared by mechanical alloying of powders.

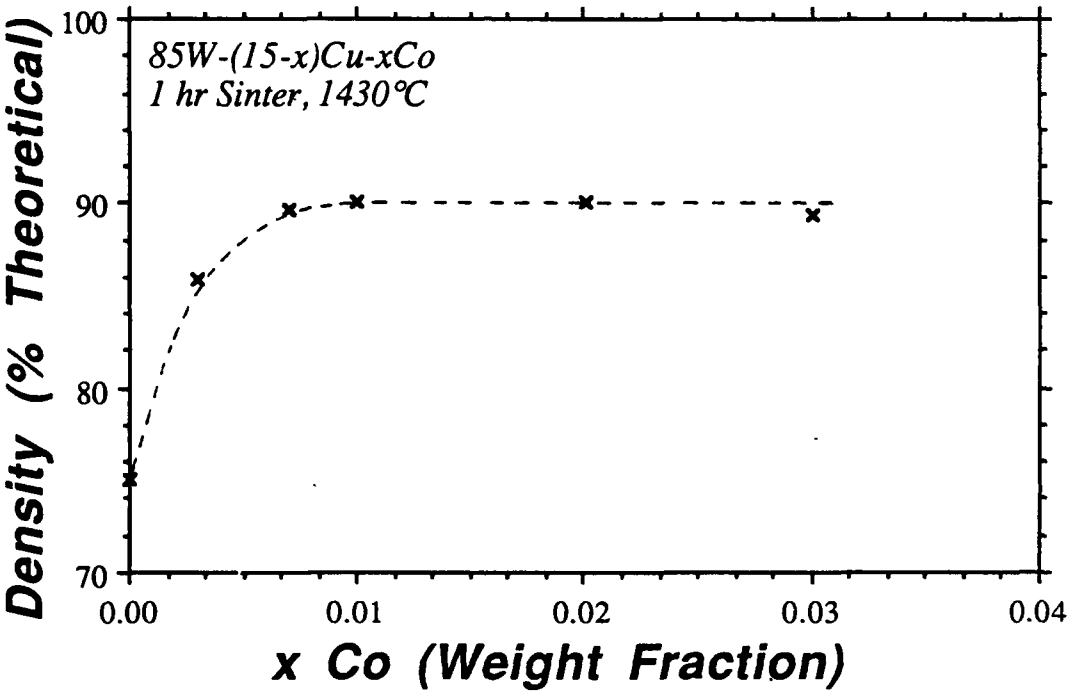

Figure 17
Effect of Co addition and sintering parameters on the as-sintered density.

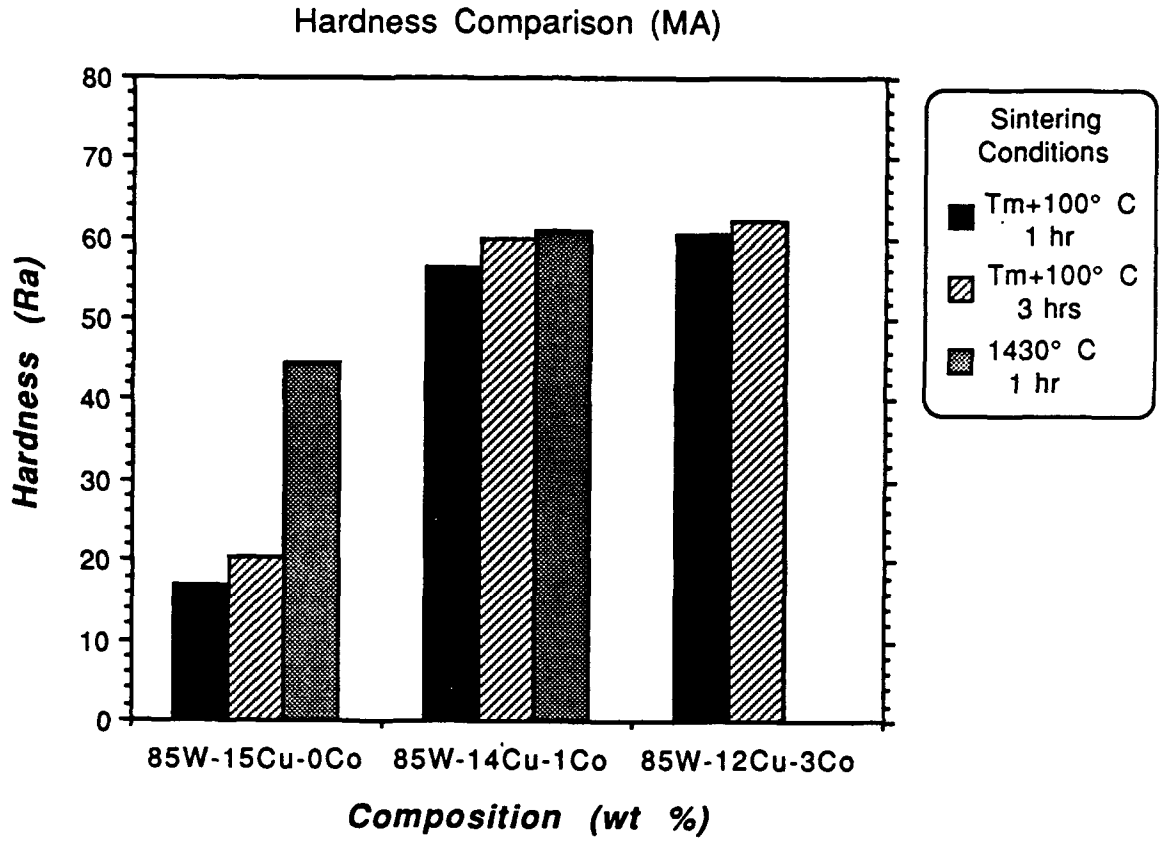

Figure 18
Effect of Co addition and sintering parameters on the as-sintered hardness. The hardness is affected by the sintering parameters as well as the Co addition.

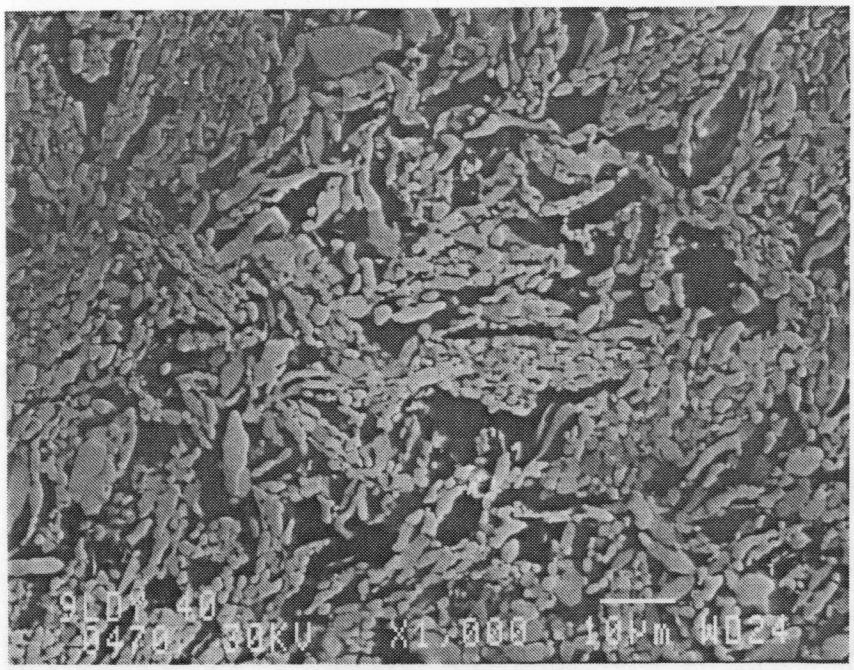

Figure 19
85W-15Cu, prepared by mechanical alloying, sintered at 1430°C for 1 hr. The W platelet structure is recrystallized into distinct grains but spheroidization is limited.

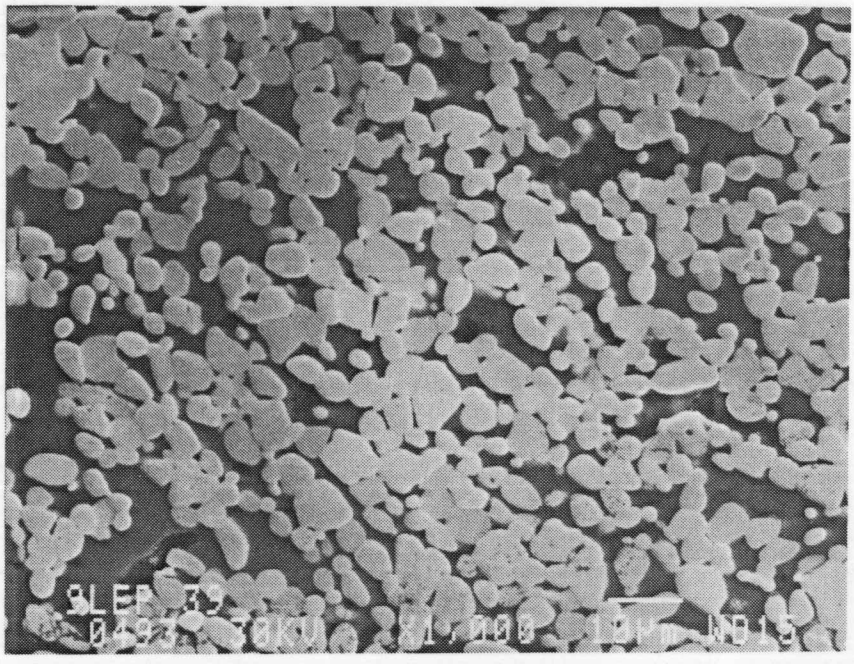

Figure 20
85W-14Cu-1Co, prepared by mechanical alloying, sintered at 1430°C for 1 hr. The W grains have coarsened and are more spheroidized due to the Co addition.

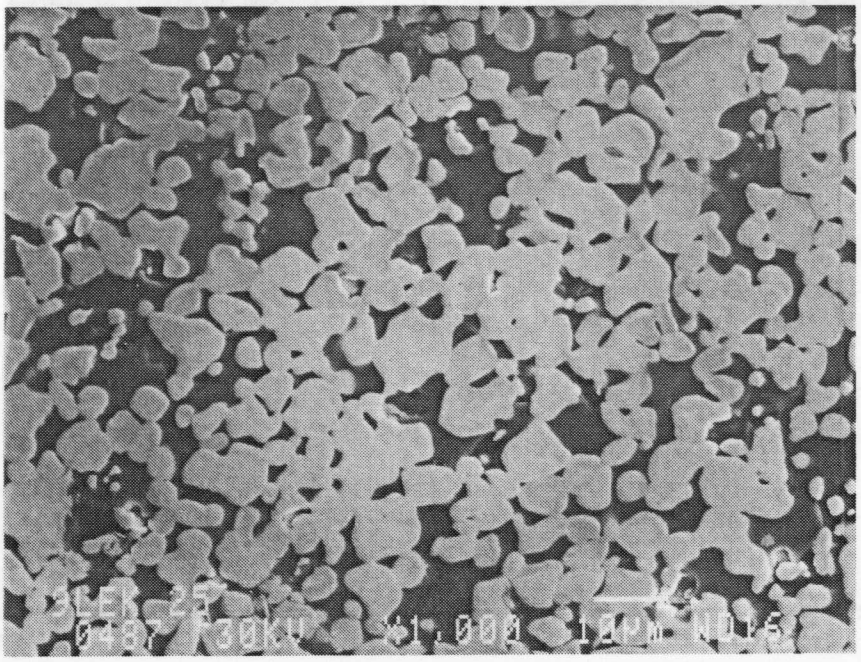

Figure 21
85W-12Cu-3Co, prepared by mechanical alloying, sintered at 1430°C for 1 hr. Grain growth and W platelet spheroidization have completely erased all signs of the mechanically alloyed platelet structure.

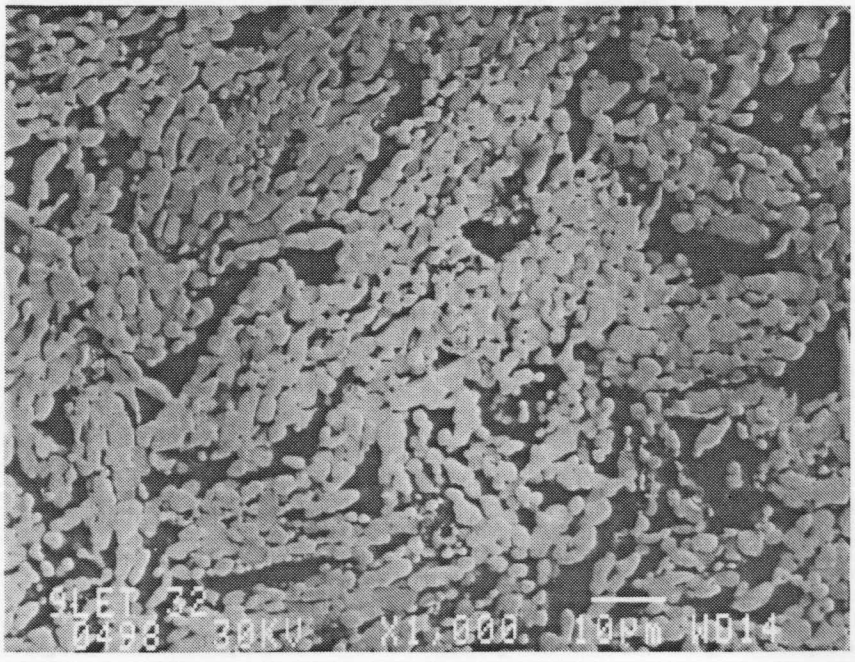

Figure 22
85W-14Cu-1Co, prepared by mechanical alloying, sintered at 1280°C for 1 hr. Compare with Figure 11. Lower sintering temperature results in less grain growth and less W particle spheroidization.

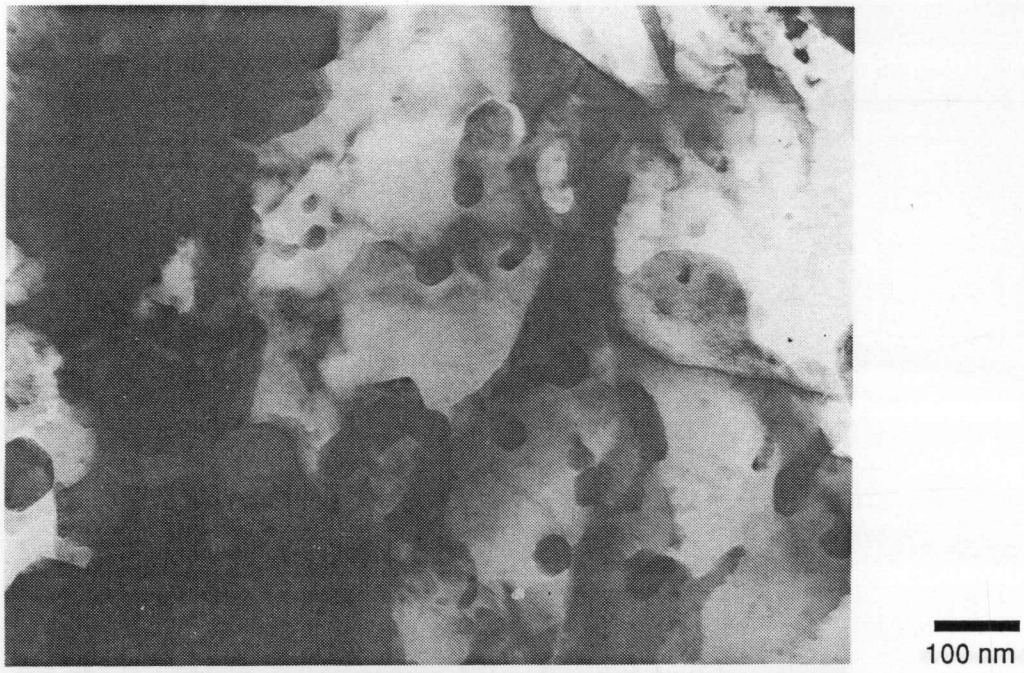

Figure 23
TEM micrograph from specimen consisting of Cu+Co liquid deposited onto a W substrate at 1430°C. Dark particles are Co-rich precipitates in the Cu matrix.

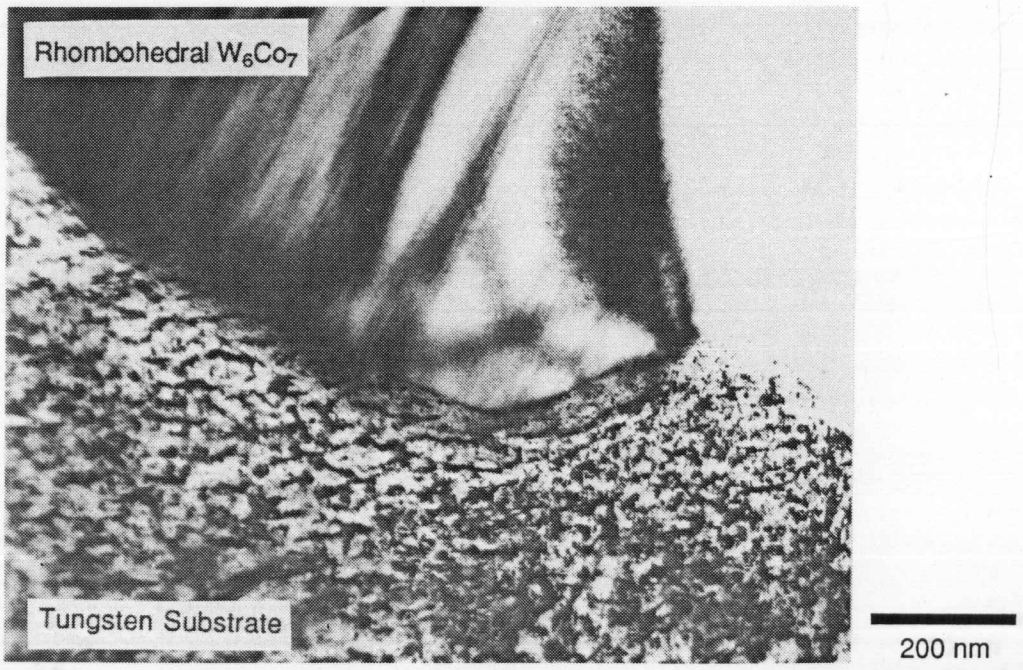

Figure 24
TEM micrograph from specimen consisting of Cu+Co liquid deposited onto a W substrate at 1430°C. Shown is a thick deposit of the W_6Co_7 phase on the W sheet.

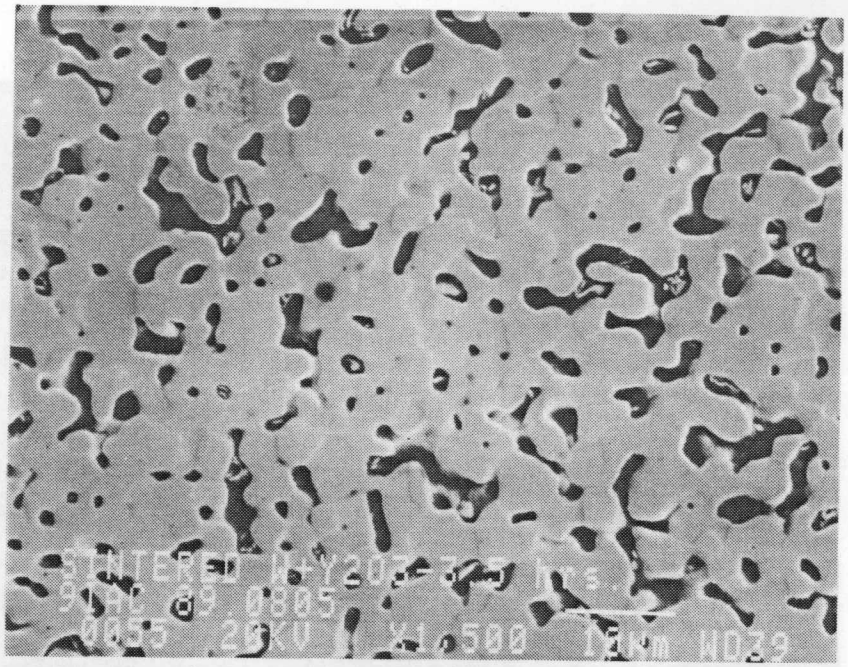

Figure 25
W+1.4% (vol) Y_2O_3 cold compacted and sintered at 1900° C in H_2 for 3.5 hrs.

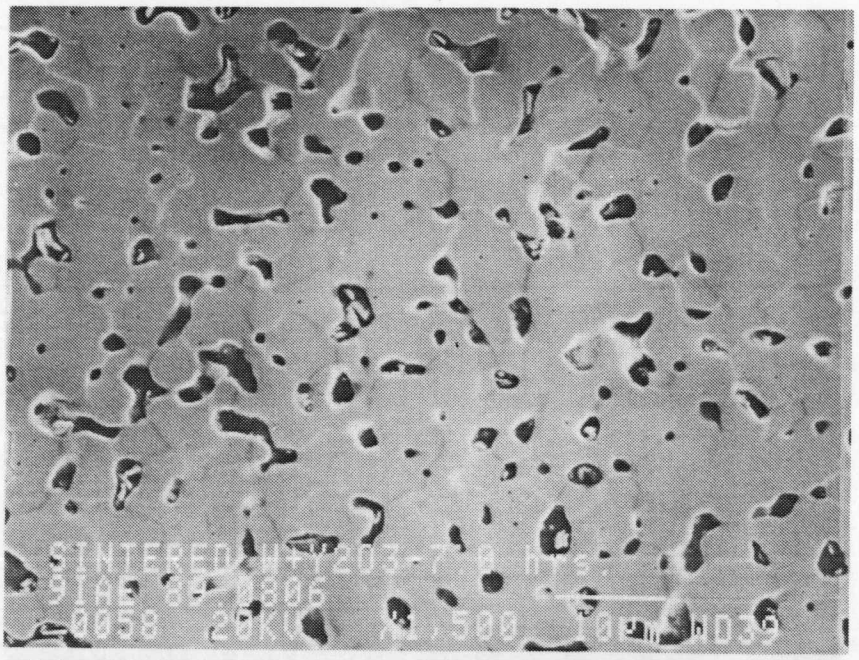

Figure 26
W+1.4% (vol) Y_2O_3 cold compacted and sintered at 1900° C in H_2 for 7 hrs. Grain growth is observed with longer sintering times and microstructure remains porous.

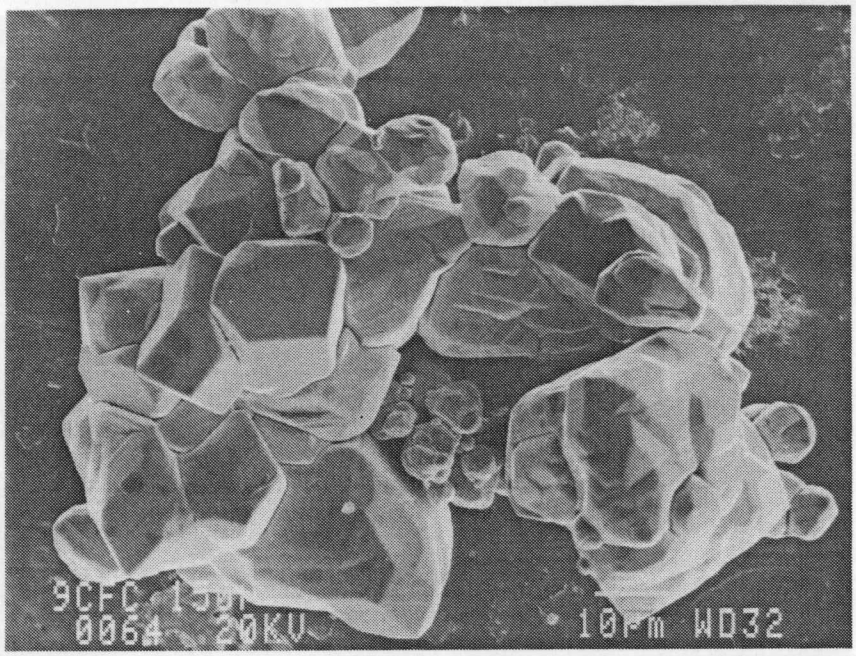

Figure 27
SEM micrograph of 150 µm W powder. Large particles appear to be an agglomeration of finer particles.

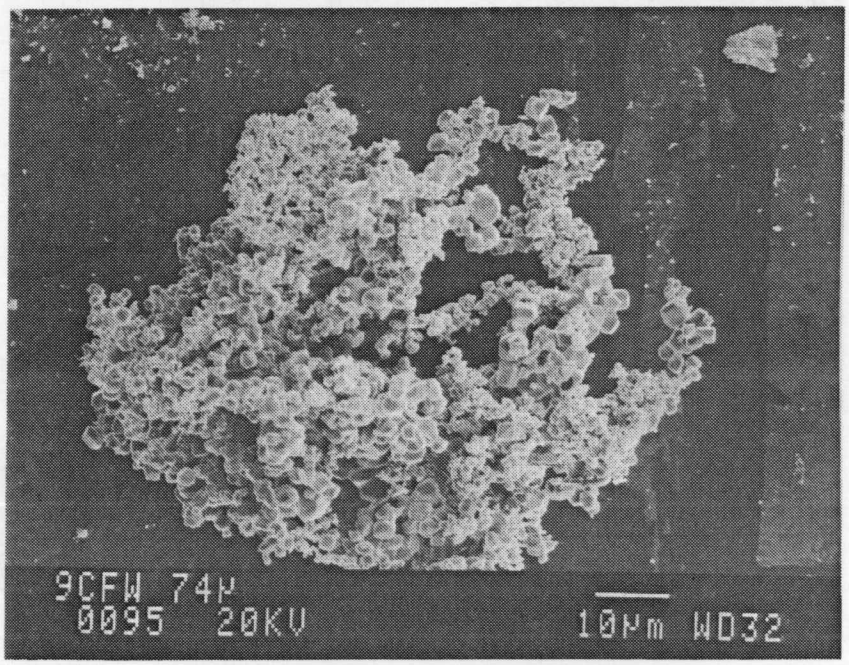

Figure 28
SEM micrograph of 74 µm W powder. Large powder particles are actually an agglomeration of much finer W grains.

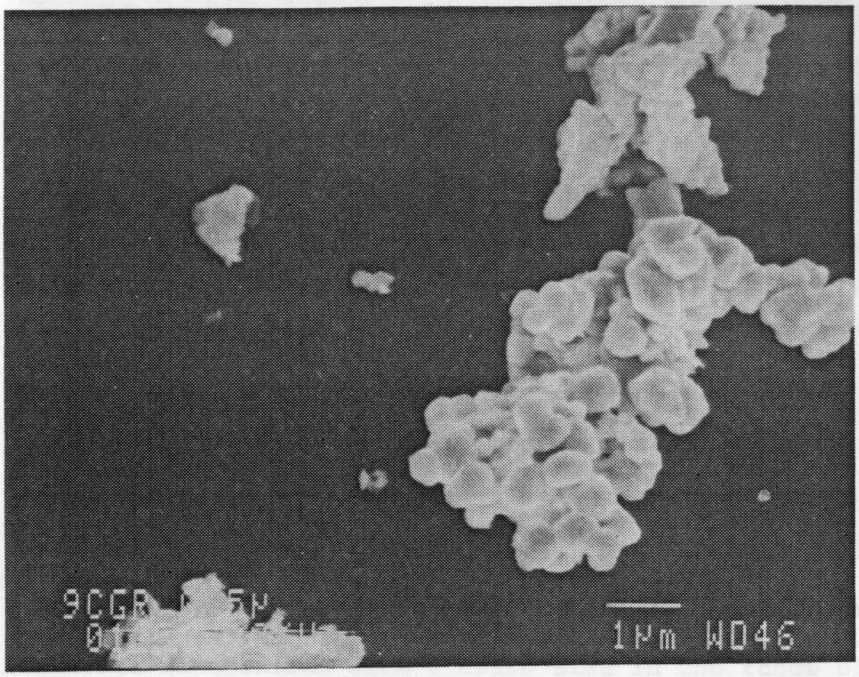

Figure 29
SEM micrograph of 0.5 µm powder.

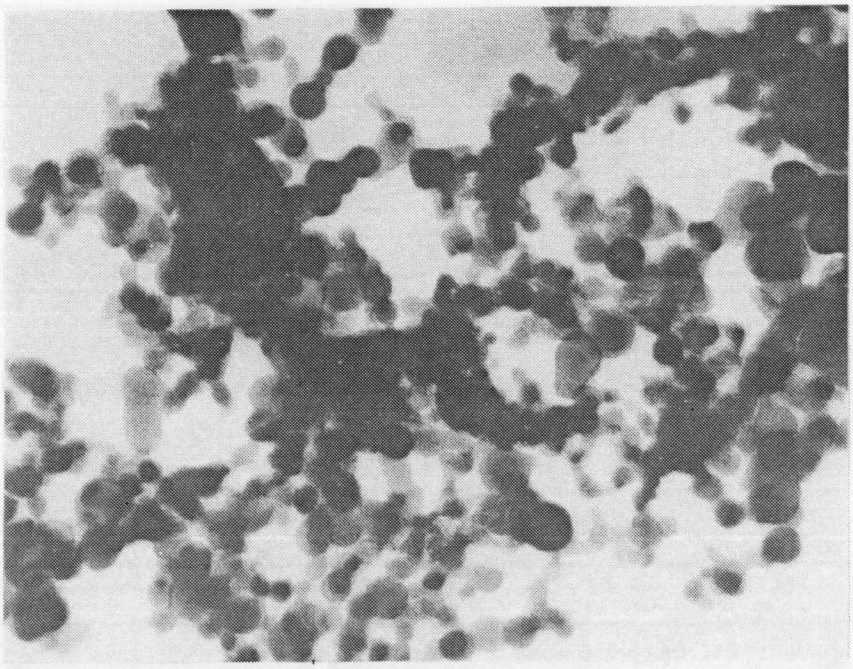

Figure 30
Ultrafine W powder obtained from Sumitomo (Japan). Individual W particles, just at the edge of the magnification capabilities of the SEM, have a size in the range of 0.02-0.03 µm (20-30 nanometers).

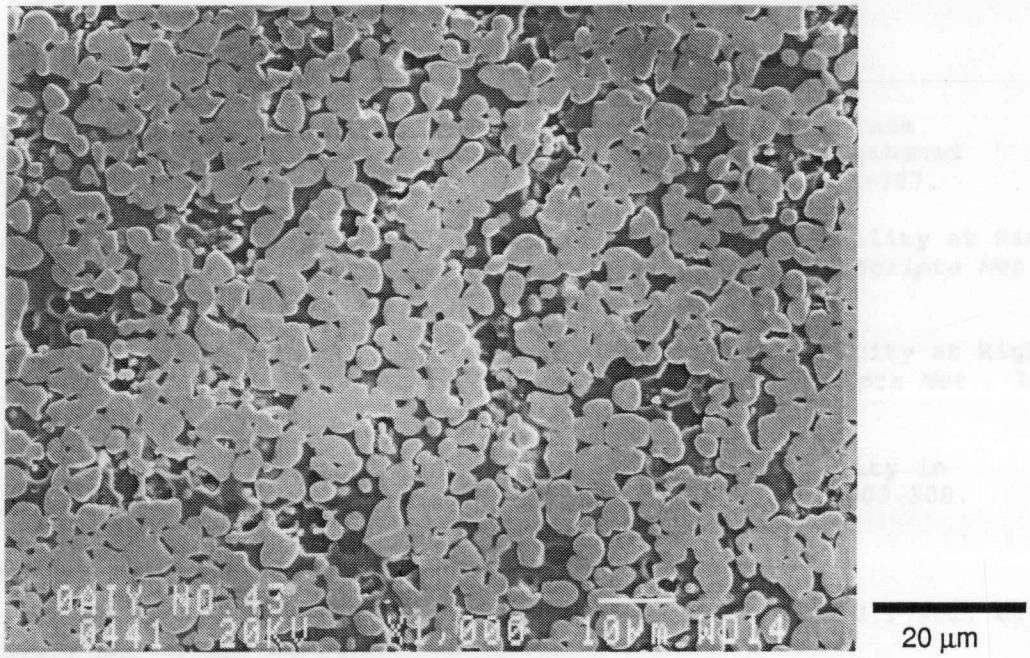

Figure 31
SEM micrograph of 85W-12Cu-3Co material, prepared from 0.5 µm W powder, mechanically alloyed, and sintered at 1430°C for 1 hr. Fine, equiaxed grain structure is obtained with a grain size in the range of 5-10 µm.

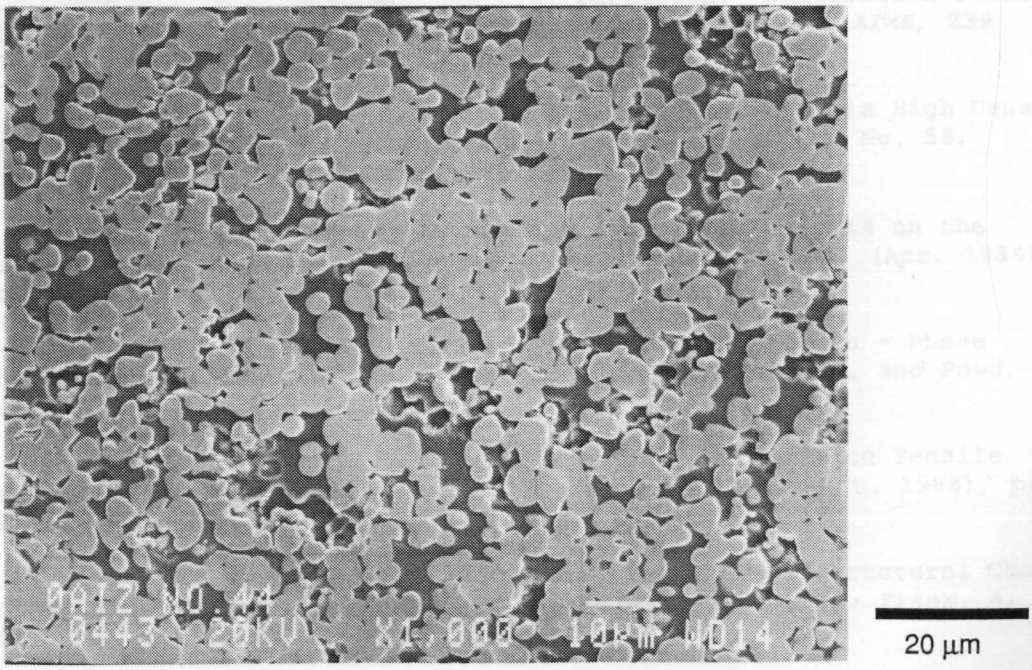

Figure 32
SEM micrograph of 85W-12Cu-3Co material, prepared from 0.02 µm W powder, mechanically alloyed, and sintered at 1430°C for 1 hr. Fine, equiaxed grain structure is obtained with a grain size in the range of 2-5 µm.

5.0 References

1. J.K. Gregory, J.C. Gibeling, and W.D. Nix, "High Temperature Deformation of Ultra-Fine-Grained Oxide Dispersion Strengthened Alloys", *Metall. Trans. A,* **16A** (4), (May, 1985), pp. 777-787.

2. T.G. Nieh, P.S. Gilman, and J. Wadsworth, "Extended Ductility at High Strain Rates in a Mechanically Alloyed Aluminum Alloy", *Scripta Met.,* **19**, (1985), pp. 1375-1378.

3. T.G. Nieh, C.A. Henshall, and J. Wadsworth, "Superplasticity at High Strain Rates in a SiC Whisker Reinforced Al Alloy", *Scripta Met.,* **18**, (1984), pp. 1405-1410.

4. M. Garfinkle, W.R. Witzke, and W.D. Klopp, "Superplasticity in Tungsten-Rhenium Alloys", *Trans. AIME,* **245** (1969), pp. 303-308.

5. Binary Alloy Phase Diagrams, ASM, (1987)

6. Y. Muramatsu and T. Takeda, *J. Japan Society Powd. Metall.,* vol. 23 (1976), No. 1, pp. 20-24.

7. M. Hansen, Constitution of Binary Alloys, McGraw-Hill, (1958).

8. R. Kieffer, K. Sedlatschek, and H. Braun, "Tungsten Alloys of High Melting Point", *J of Less Common Met,* **1**, No. 1, (Feb. 1959), pp. 19-33.

9. J.E. Spruiell, B.F. Schuler, and F.H. Patterson, "Deformation Studies of Thermomechanically Deposited Tungsten Sheet",*Trans. AIME,* **239** (Nov.1969), pp. 1763-1767.

10. E.C. Green, D.J. Jones, and W.R. Pitkin, "Developments in High Density Alloys", Symposium in Powder Metallurgy: Special Report No. 58, (1954), The Iron and Steel Institute, p. 253.

11. R.M. German and K.S. Churn, "Sintering Atmosphere Effects on the Ductility of W-Ni-Fe Heavy Metals", *Met. Trans. A,* **15A**, (Apr. 1984), pp. 747-754.

12. C.J. Li and R.M. German, "Enhanced Sintering of Tungsten - Phase Equilibria Effects on Properties", *Int. J. Powd. Metall. and Powd. Tech.,* **20** (2), (1984), pp. 149-162.

13. A. Bose and R.M. German, "Sintering Atmosphere Effects on Tensile Properties of Heavy Alloys", *Metall. Trans. A,* **19A**, (Oct. 1988), pp. 2467-2476.

14. J.K. Park, S.L. Kang, K.Y. Eun, and D.N. Yoon, "Microstructural Change during Liquid Phase Sintering of W-Ni-Fe Alloy", *Metall. Trans. A,* **20A**, (May 1989), pp. 837-845.

15. R.M. German, L.L. Bourguignon, and B.H. Rabin, "Microstructure Limitations of High Tungsten Content Heavy Alloys", *J. of Metals,* **37** (8), (Aug. 1985), pp. 36-39.

16. G. Price, C.J. Smithels, and S.V. Williams, *J. Inst. of Metals,* **62,** (1938), pp. 239-247.

17. N.C. Kothari, *J. Less Common Metals,* **13,** (1967), pp. 457-468.

18. W.D. Kingery, "Densification during Sintering in the Presence of a Liquid Phase. I. Theory", *J. Appl. Physics,* **30** (3), (Mar. 1959), pp.301-306.

19. W.D. Kingery, "Densification during Sintering in the Presence of a Liquid Phase. II. Experimental", *J. Appl. Physics,* **30** (3), (Mar. 1959), pp.307-310.

20. A. Bose and R.M. German, "Microstructural Refinement of W-Ni-Fe Heavy Alloys by Alloying Additions", *Metall. Trans. A,* **19A,** (Dec. 1988), pp. 3100-3103.

21. B.H. Rabin and R.M. German, "Microstructure Effects on Tensile Properties of Tungsten-Nickel-Iron Composites", *Metall. Trans. A,* **19A,** (June 1988), pp. 1523-1532.

22. J. Lankford and S.R. Bodner, "Fracture of Tungsten Heavy Alloys Under Impulsive Loading Conditions", *J. Mater. Sci. Letters,* **7,** (1988), pp. 1355-1358.

23. Binary Alloy Phase Diagrams Vol. 1, Thaddeus B. Massalski, Ed., Amer. Society for Metals, Metals Park, Ohio, 1986.

24. I.H. Moon and J.H. Lee "Activated Sintering of Tungsten-Copper Contact Materials", *Powd. Met.,* **1,** (1979), pp. 5-7.

25. Randall M. German, Liquid Phase Sintering, Plenum Press, New York, NY, (1985).

26. R. Warren and M.B. Waldron, "Microstructural Development During the Liquid Phase Sintering of Cemented Carbides I: Wetability and Grain Contact", *Powder Met.,* **15,** (1972), pp. 166-180.

27. O.K. Riegger and L.H. Van Vlack, "Dihedral Angle Measurement", *Trans. TMS-AIME,* **218,** (1960), pp. 933-935.

28. C.C. Koch, "Materials Synthesis by Mechanical Alloying", *Ann. Rev. Mater. Sci.,***19,** (1989), pp. 121-143.

29. H.C. Lee and J. Gurland, "Hardness and Deformation of Cemented Tungsten Carbide", *Mater. Sci. and Engr.,* **33** (1), (Apr. 1978), pp. 125-132.

30. R.B. Heady and J.M. Cahn: *Metall. Trans. A,* 1970, vol. 1, pp. 185-189.

31. W.J. Huppmann and H. Riegger: *Acta Met.,* 1975, vol. 23, pp. 965-971.

32. V.N. Eremenko, Y.V. Naidich, and I.A. Lavrinenko: *Liquid Phase Sintering,* 1970, Consultants Bureau, New York, NY.

33. J.M. Cahn and R.B. Heady: *J. Amer. Cer. Soc.,* 1970, vol. 53, pp. 406-409.

34. W.W. Mullins, "Grain Boundary Grooving by Volume Diffusion", *Trans. TMS-AIME*, **218**, (Apr. 1960), pp. 354-361.

35. L.D. Graham and R.W. Kraft, "Coarsening of Eutectic Microstructures at Elevated Temperatures", *Trans. TMS-AIME*, **236**, (Jan. 1966), pp. 94-102.

36. R.M. German, Powder Metallurgy Science, Metal Powder Industries Federation, Princeton, NJ, (1984).

37. J. Wittenauer, Unpublished Research Results, June, 1989.

38. V.A. Phillips, "Electron-Microscope Observations on Precipitation in a Cu-3.1 wt Pct Co Alloy", *Trans. TMS-AIME*, **230**, (Aug. 1964), pp. 967-976.

39. A.L. Prill, H.W. Hayden, and J.H. Brophy, "The Role of Phase Relationships in the Activated Sintering of Tungsten", *Trans. TMS-AIME*, **230**, (June, 1964), pp. 769-772.